Induction of Mutant Dynamin Specifically Blocks Endocytic Coated Vesicle Formation

Hanna Damke, Takeshi Baba, Dale E. Warnock, and Sandra L. Schmid

Department of Cell Biology, The Scripps Research Institute, La Jolla, California 92037

Abstract. Dynamin is the mammalian homologue to the *Drosophila shibire* gene product. Mutations in this 100-kD GTPase cause a pleiotropic defect in endocytosis. To further investigate its role, we generated stable HeLa cell lines expressing either wild-type dynamin or a mutant defective in GTP binding and hydrolysis driven by a tightly controlled, tetracycline-inducible promoter. Overexpression of wild-type dynamin had no effect. In contrast, coated pits failed to become constricted and coated vesicles failed to bud in cells overexpressing mutant dynamin so that endocytosis via both transferrin (Tfn) and EGF receptors was potently inhibited. Coated pit assembly, invagination, and the recruitment of receptors into coated pits were unaffected. Other vesicular transport pathways, including Tfn receptor recycling, Tfn receptor biosynthesis, and cathepsin D transport to lysosomes via Golgi-derived coated vesicles, were unaffected. Bulk fluid-phase uptake also continued at the same initial rates as wild type. EM immunolocalization showed that membrane-bound dynamin was specifically associated with clathrin-coated pits on the plasma membrane. Dynamin was also associated with isolated coated vesicles, suggesting that it plays a role in vesicle budding. Like the *Drosophila shibire* mutant, HeLa cells overexpressing mutant dynamin accumulated long tubules, many of which remained connected to the plasma membrane. We conclude that dynamin is specifically required for endocytic coated vesicle formation, and that its GTP binding and hydrolysis activities are required to form constricted coated pits and, subsequently, for coated vesicle budding.

DYNAMIN is a member of a structurally related but functionally heterogeneous family of GTPases that itself exhibits an apparently diverse array of functional properties in vitro (reviewed by Collins, 1991; Vallee, 1992). Originally isolated as a nucleotide-dependent microtubule-bundling protein (Shpetner and Vallee, 1989; Scaife and Margolis, 1990), dynamin was later shown to have microtubule-stimulated GTPase activity (Shpetner and Vallee, 1992; Maeda et al., 1992). Recently, other factors have been shown to regulate dynamin GTPase activity in vitro through interaction with its 100-aa basic and proline-rich COOH-terminal domain (Gout et al., 1993; Herskovits et al., 1993*b*). These include acidic phospholipids (Tuma et al., 1993) and a subset of SH3 domain–containing proteins, including Grb2, P85-α, phospholipase Cγ, c-*fyn*, and c-*src* (Gout et al., 1993; Herskovits et al., 1993*b*). The significance between these in vitro interactions and dynamin's function in vivo has not been established.

Much of what is known about the function of dynamin in vivo comes from phenotypic analysis of a mutation in a *Drosophila* homologue to mammalian dynamin called *shibire*^{ts} (Chen et al., 1991; van der Bliek and Meyerowitz, 1991). The most dramatic phenotype associated with *shibire* flies is temperature-sensitive paralysis (Grigliatti et al., 1973). Ultrastructural analysis of the nerve terminals from *shibire* flies after shift to the nonpermissive temperature revealed a rapid loss of synaptic vesicles and an accumulation of both coated and uncoated invaginations at the synaptic membrane (Poodry and Edgar, 1979; Kosaka and Ikeda, 1983*a*; Koenig and Ikeda, 1989). These results suggested a direct role for the *shibire* gene product in synaptic vesicle recycling, although it has not been localized to the endocytic structures that accumulate at the nonpermissive temperature. Subsequent analysis of a number of tissues (Kosaka and Ikeda, 1983*b*; Kessell et al., 1989; Koenig and Ikeda, 1990; Tsuruhara et al., 1990) revealed that the *shibire* mutation caused a pleiotropic defect in endocytosis.

The fact that mutations in *shibire* affect endocytosis in all tissues examined is of interest since mRNAs encoding dynamin-1, the originally identified mammalian homologue of *shibire*, are exclusively expressed in neurons (Nakata et al., 1991; van der Bliek et al., 1993; Cook et al., 1994; Sontag et al., 1994). A second isoform of mammalian dynamin, referred to as dynamin-2, which encodes a ubiquitously expressed protein 79% identical to dynamin-1 and 66% identical to *shibire* was recently identified (Cook et al., 1994; Sontag et al., 1994). It has not yet been established whether dynamin-2 homologue is also involved in endocytosis, or

Address all correspondence to Sandra L. Schmid, Department of Cell Biology, The Scripps Research Institute, 10666 N. Torrey Pines Road, La Jolla, CA 92037. Phone: (619) 554-2311; fax: (619) 554-6253.

is instead involved in other intracellular vesicle budding events.

That dynamin-1 is, in fact, a functional homologue of the *shibire* gene product was established by demonstrating that receptor-mediated endocytosis was blocked in mammalian cells transiently expressing dominant-interfering mutants of the neuronal isoform of dynamin (van der Bliek et al., 1993; Herskovits et al., 1993*a*). Receptor-mediated endocytosis occurs via a number of distinct intermediates that have been identified using combined biochemical and morphological approaches (reviewed in Schmid, 1993). Early stages of coated vesicle formation involve the assembly of the coat proteins, AP2 complexes, and clathrin, from cytosolic pools onto the plasma membrane and the recruitment of receptors into coated pits (Mahaffey et al., 1990; Smythe et al., 1992*a*; Lamaze et al., 1993). Originally planar clathrin lattices (Heuser and Evans, 1980) then invaginate in an apparently spontaneous process (Moore et al., 1987; Smythe et al., 1989). An as yet undefined, but active process leads to constriction of the neck of coated pits so as to selectively sequester receptor-bound, biotinylated ligands from interaction with exogenously added avidin or other bulky probes (Schmid and Carter, 1990; Schmid and Smythe, 1991; Carter et al., 1993). Ligands sequestered in these constricted coated pits remain accessible to small probes such as the membrane impermeant reducing agent, β-mercaptoethanesulfonic acid. Finally, budding is completed by an ATP- and GTP-dependent membrane fission event, and receptor-bound ligands are internalized into sealed coated vesicles (Schmid and Smythe, 1991; Carter et al., 1993). We previously found that overexpression of a predicted GTPase-defective mutant of dynamin, but not wild-type (wt)[1] dynamin, blocked endocytosis at a stage after coat assembly and before the sequestration of receptor-bound ligands into constricted coated pits (van der Bliek et al., 1993).

The intermediate stage in coated vesicle formation blocked by expression of the dynamin mutant is not known to require either microtubule (MT) or SH3 domain–containing proteins involved in signal transduction. Thus, it remains difficult to reconcile the requirement for dynamin function in vivo with the functional interactions between dynamin and MTs or SH3 domain–containing proteins documented in vitro. Therefore, we sought other possible functions of dynamin that might explain these in vitro interactions by further investigating the role of dynamin in vivo. To this end, stably transformed cell lines that express wt and mutant dynamin under the control of an inducible, tightly regulated promoter were established. Using these cells, we have conducted a detailed biochemical and morphological analysis of the functional consequences of overexpression of a dynamin mutant defective in GTP binding and hydrolysis. We conclude that dynamin is specifically targeted to coated pits at the plasma membrane, where it is required for coated pit constriction and coated vesicle budding.

1. *Abbreviations used in this paper*: AEBSF, [4-(2-aminoethyl)-benzenesulfonfluoride; BEGF, biotinylated EGF; BSST, biotinylated transferrin; D65-gold, gold-conjugated D65 anti-human transferrin receptor mAbs; elel, element 1; HA, hemmaglutinin; MT, microtubule; Tfn, transferrin; Tfn-R, transferrin receptor; tet, tetracycline; TGN, *trans*-Golgi network; tTA, chimeric transactivator; wt, wild type.

Materials and Methods

Antibodies

Anti-human transferrin (Tfn) receptor polyclonal serum and monoclonal antibodies (HTR.D65 and B3/25) were a kind gift of I. S. Trowbridge and S. White (Salk Institute, La Jolla, CA). Anti-cathepsin D antiserum was from T. Braulke (University of Göttingen, Göttingen, Germany). Anti-β/β'-adaptin monoclonal antibody 100/1 (Ahle et al., 1988) was generously provided by Sigma Chemical Co. (St. Louis, MO). The monoclonal anti-hemagglutinin-tag antibody, 12CA5, was provided by R. A. Lerner (The Scripps Research Institute, La Jolla, CA). Mouse monoclonal anti-clathrin IgM antibody CHC 5.9 was obtained from IBL Research Products (Cambridge, MA). Anti-vinculin monoclonal antibody was a generous gift from Vito Quaranta (The Scripps Research Institute, La Jolla, CA). Polyclonal anti-tubulin antibody was obtained from ICN Immunochemicals (Irvine, CA). Rhodamine-phalloidin and Texas red–conjugated goat anti-mouse antibody were obtained from Molecular Probes, Inc. (Eugene, OR). FITC-conjugated goat anti-mouse IgG (γ chain specific) and Texas red–conjugated goat anti-mouse IgG (μ chain specific) were obtained from Calbiochem-Novabiochem Corp. (La Jolla, CA). FITC-conjugated goat anti-rabbit IgG was obtained from Organon Teknika-Cappel (Durham, NC). Colloidal gold (5 nm)–conjugated goat anti-mouse IgG was obtained from Ted Pella Inc. (Redding, CA). All primary monoclonal antibodies were purified by affinity chromatography on protein G–Sepharose (Pierce Chemicals Co., Rockford, IL).

Other Reagents

Human diferric transferrin (Tfn) and biotinylated receptor grade mouse EGF were from Boehringer-Mannheim Biochemicals (Indianapolis, IN). Tfn was biotinylated as previously described (Smythe et al., 1992*b*). Omnisorb cells, pronase and [4-(2-aminoethyl)-benzenesulfonylfluoride, HCl] (AEBSF) were from Calbiochem-Novabiochem Corp. Tran^{35}S-label™ (1 mCi/μmol) was from ICN Biomedicals, Inc. Reagent-grade chemicals were obtained from Sigma Chemical Co. or Boehringer Mannheim Biochemicals, unless otherwise specified.

Cells

The stable HeLa cell line, designated HtTA, expressing the chimeric tetracycline regulatable transcription activator was generously provided by H. Bujard (Zentrum für Molekulare Biologie, Heidelberg, Germany). Cells were cultured in DME supplemented with 10% (vol/vol) fetal bovine serum, 100 U/ml each of penicillin and streptomycin, and 400 μg/ml active G418 (Geneticin; GIBCO BRL, Gaithersburg, MD).

Preparation of cDNA Constructs

The cDNAs for wild-type and the elel mutant of dynamin were subcloned from the modified vaccinia expression constructs pTM1-Hwt and pTM1-elel described previously (van der Bliek et al., 1993) into the tetracycline-inducible expression plasmid pUHD10-3 (generously provided by H. Bujard). This plasmid contains seven repeat units of the *Escherichia coli* tetracycline operator linked to a cytomegalovirus (CMV) minimal promoter directly upstream of the cloning site (Gossen and Bujard, 1992; Resnitzky et al., 1994). To add an hemagglutinin (HA) epitope at the NH_2 terminus of the dynamin cDNAs, a digest with SpeI/Bgl II was performed to remove a small fragment at the 5' end of the coding sequence. This fragment was replaced by a 76-bp synthetic SpeI/Bgl II linker (CTAGTGGATCCAAGGAGCCGCCGCCATGGAGTATGATGTTCCTGATTATGCTCATATGGGCAACCGCGGCATGGAA), which provided the start codon preceding the hemagglutinin tag coding sequence of 30 bp (underlined) (Wilson et al., 1984). The first 200 bp of the modified constructs were confirmed by DNA sequencing. For subcloning of the full-length cDNAs corresponding to HA-wt dynamin and HA-elel dynamin, a 3.2-kbp SpeI/SalI fragment was blunt end ligated into the XbaI site of the plasmid pUHD10-3. After subcloning, the sequence of the region spanning the insertion site was confirmed.

Generation of Stably Transformed Cells

The generation of stably transformed HeLa cells with tightly regulated expression of wt and mutant dynamin will be described in detail elsewhere (Damke et al., 1995). Briefly, a 60-mm plate seeded with 5×10^5 HtTA cells was transfected with cDNA (10 μg) encoding the wt or elel mutant

dynamin under the control of the tTA-responsive promoter along with the plasmid pBSpac (0.5 μg), containing the puromycin resistance gene (de la Luna et al., 1988), using calcium phosphate precipitation as described (Sambrook et al., 1989). Plasmid pUHD10-3 without dynamin cDNA was used to generate mock-transformed cells. Positive clones were selected and cultured with 200 ng/ml puromycin, 400 μg/ml G418, and 2 μg/ml tetracycline (tet). Puromycin-resistant clones were screened for their ability to express dynamin 48 h after induction in the absence of tet by SDS-PAGE and Western blot analysis. For experiments, subconfluent cultures were split by trypsin/EDTA dispersion and (1.2×10^6) cells were plated on 100-mm culture dishes in the presence (uninduced) or absence (induced) of tet ~48 h before use. At this point, the cells were ≤80% confluent.

Assay for Dynamin GTPase Activity

The expression and purification of recombinant dynamin using the baculovirus expression system in Sf9 cells will be described elsewhere (Warnock, D. E., J. L. Terlecky, and S. L. Schmid, manuscript submitted for publication). Briefly, BamHI/HindIII full-length cDNA fragments encoding wild-type and elel human neuronal dynamin were subcloned into the polycloning site of the pBlueBacIII baculovirus expression vector (Invitrogen, San Diego, CA). Recombinant baculovirus was plaque purified and amplified according to the instruction manual provided with the baculovirus expression vector system. For purification of wt and elel dynamin, Sf9 cells (1.5×10^6 cells/ml) were infected with high titer virus stocks at ~10 pfu/cell, and were harvested 48–60 h after infection. Dynamin was purified to >95% homogeneity from the cytosolic fraction by sequential Q-Sepharose and phosphocellulose chromatographic steps.

GTPase assays were performed as described by Gout et al. (1993) in 50 mM Tris-HCl, pH 7.4, 5 mM $MgCl_2$, 1 mM $MnCl_2$ in a final volume of 20 μl. Assays contained 0.25 μg wt or 1 μg elel dynamin with or without 0.1 mg/ml taxol-stabilized microtubules. Reactions were initiated by the addition of 100 μM GTP (0.1 μCi [α-^{32}P]GTP) (Amersham Corp., Arlington Heights, IL). 1.5-μl aliquots were removed at each time point and spotted onto cellulose polyethyleneimine thin-layer chromatography plates with fluorescent indicator (J. T. Baker, Inc., Phillipsburg, NJ). Nucleotides were resolved by thin-layer chromatography in 1 M $LiCl_2$/2 M formic acid (1:1). Quantitation of nucleotides, identified by comigration with known standards, was performed on a phosphorimager (Molecular Dynamics Inc., Sunnyvale, CA).

Western Blot Analysis

Cells were washed twice with PBS and lysed by the addition of 1% Triton X-100 in PBS containing 5 mM $MgCl_2$ and 1 mM AEBSF. The samples were pelleted to remove the nuclei, precipitated with 10% TCA, washed with ice-cold acetone, and solubilized in Laemmli sample buffer. Alternatively, for rapid processing of multiple samples, PBS/5 mM EDTA-detached cells were immediately lysed in 1× Laemmli sample buffer. Cell lysates were analyzed by SDS-PAGE on 7.5% gels, and were electroblotted to Immobilon-P nitrocellulose (Millipore Corp., Bedford, MA) by standard methods (Burnette, 1981). Nonspecific protein binding was blocked with 2% nonfat dry milk powder in Tris-buffered saline containing 0.1% Tween 20. The blots were incubated with the primary anti-dynamin antibody, hudy-1, at 0.1 μg/ml, or with the anti-HA-tag antibody, 12CA5, at 2.5 μg/ml, followed by detection with an alkaline phosphatase–conjugated secondary goat anti-mouse antibody (Pierce Chemical Co.), and were developed with an alkaline phosphatase color development kit (Bio-Rad Laboratories, Hercules, CA). When analyzing transferrin receptor distribution, cell lysates were resolved by SDS-PAGE 10% gels, and were then transferred to Immobilon-P. Antigen-antibody complexes were visualized using horseradish peroxidase–conjugated goat anti-rabbit antibody and the enhanced chemiluminescence (ECL) detection kit (Amersham Corp.), following the manufacturer's instructions.

Internalization Assays

Internalization assays using biotinylated transferrin (BSST) and biotinylated EGF (BEGF) were performed as previously described (van der Bliek et al., 1993; Lamaze et al., 1993), except that incubations were at 32°C to slow down the internalization process.

Assays for Intracellular Trafficking of Transferrin Receptors

Recycling from the Endosomal Compartment. Cells were incubated on 100-mm dishes for 60 min at 37°C with 8 μg/ml biotinylated Tfn to reach equilibrium labeling. Plates were transferred to ice, washed several times with cold PBS, and surface-associated biotinylated Tfn was masked with 50 μg/ml avidin for 15 min at 4°C. Avidin was quenched with biocytin (5 μg/ml). The cells were then harvested from the plates by a 5-min incubation at 4°c with PBS/5 mM EDTA, and were collected by centrifugation at 1,000 *g* for 5 min. Cells were resuspended at 4°C in PBS^{++} containing 0.2% BSA, 2 μg/ml nonbiotinylated Tfn, and 5 mM glucose, and were returned to 37°C for the indicated times. Biotinylated Tfn that recycled to the cell surface during reincubation was again masked with avidin, and the cells were treated exactly as described for endocytosis assays. Results are expressed as the percent of initial intracellular B-Tfn that remains inaccessible to avidin during reincubation.

Trafficking along the Biosynthetic Pathway. Cells were pulse-labeled for 15 min in methionine-free media containing 150 μCi/ml ^{35}S-Tran ^{35}S-label™ (ICN Biomedicals, Inc., Costa Mesa, CA). Incorporation was terminated by washing the cells twice with PBS and chase periods of ≤4 h were initiated by addition of prewarmed complete DME containing 10% fetal bovine serum. Cells were solubilized in PBS containing 1% Triton X-100 and a protease inhibitor cocktail comprised of 10 μg/ml pepstatin, antipain, and leupeptin; 12.5 IU/ml aprotinin A; 1% BSA; 1 mM AEBSF; and 2 mg/ml soybean trypsin inhibitor in 0.05% DMSO. Nuclei were removed by centrifugation (16,000 *g* for 5 min) at 4°C, and the cell lysates were brought to a final concentration of 1% Nonidet P-40, 1% sodium deoxycholate, and 0.1% SDS for immunoprecipitation with the B3/25 monoclonal anti-transferrin receptor antibody and goat anti-mouse IgG prebound to 1% (vol/vol) Omnisorb cells. Transport through the Golgi apparatus was determined by acquisition of resistance to endoglycosidase H and addition of complex oligosaccharides as previously described (Omary and Trowbridge, 1981). To detect the arrival of labeled transferrin receptor at the plasma membrane, cells on 100 mm dishes were incubated on ice with 2 ml of PBS containing 12.8 U/ml tosylamide-phenylethyl chloromethyl ketone–trypsin (12.8 U/ml). After digestion for 30 min, the protease inhibitor cocktail was added from a stock solution to the media. Both the cell pellet and the media were collected, and transferrin receptor (Tfn-R) and its trypsin-generated fragments were immunoprecipitated and analyzed by SDS-PAGE as described (Omary and Trowbridge, 1981). Gels were exposed overnight on a Molecular Dynamics phosphorimage screen and developed on the phosphorimager. For quantitation of protein bands, the Molecular Dynamics ImageQuant software was used.

Steady-state Distribution. The steady-state distribution of the Tfn-R was determined after treating unlabeled cells with trypsin as described above. Combined supernatants and cell pellets were directly solubilized in Laemmli sample buffer for analysis by SDS-PAGE on 10% polyacrylamide gels. The ratio of intracellular (~90 kD intact Tfn-R) to surface (released ~70 kD ectodomain) Tfn-R was determined after Western blotting and detection using anti-Tfn-R polyclonal serum and the enhanced chemiluminescence detection system. Quantification was performed using a digital scanning densitometer.

Immunoprecipitation of Cathepsin D

Cells were pulse labeled for 30 min and chased in complete medium for ≤4 h as described above. Cell pellets harvested after various chase times were frozen in liquid nitrogen and stored at −20°C until all time points were collected. Cell lysates were prepared and immunoprecipitation of cathepsin D was performed as described by Gieselmann et al. (1983). The appearance of the 32-kD mature form of cathepsin D, which marks its arrival in lysosomes, was determined by SDS-PAGE on 12.5% acrylamide. Radioactive bands were visualized and quantitated by phosphorimage analysis.

Fluid Phase Uptake

For the analysis of fluid phase uptake cells were grown on 35 mm plates, washed twice with PBS and incubated with 1 mg/ml HRP in DME/20 mM Hepes, 0.2% BSA, pH 7.4, for various times. The uptake was stopped by aspirating the medium followed by six washes with PBS, 1 mM $MgCl_2$, 1 mM $CaCl_2$, 0.2% BSA, pH 7.4, for 5 min at 4°C and two short washes with PBS at 4°C (Marsh et al., 1987). The cells were then treated with 0.1% pronase in PBS, pH 7.4, to detach the cells and remove any HRP nonspecifically adsorbed to the cell surface. Under these conditions, backgrounds at 4°C were undetectable over cell lysate–only blanks. Cell suspensions were then washed by pelleting through a sucrose cushion (0.5 M in PBS, pH 7.4) for 5 min at 4°C at 4,000 rpm in a refrigerated Eppendorf microfuge. The cells were solubilized in PBS, 0.5% Triton X-100, and aliquots were assayed for enzyme activity using *o*-phenylenediamine as a substrate or for protein concentration using the Micro-BCA assay (Pierce Chemical Co.).

Indirect Immunofluorescence

Transformed HtTA cells were grown in the presence or absence of tet on glass coverslips for ≥48 h to ~60% confluency. The cells were permeabilized in 40 μg/ml digitonin for 5 min, washed briefly to deplete cytosolic contents, and then fixed with 4% paraformaldehyde in 0.1 M phosphate buffer, pH 7.4, for 30 min. This and all subsequent manipulations were at room temperature. The cells were blocked in 1% BSA, 5% normal goat serum, 0.01% saponin, 0.02% sodium azide in PBS for 60 min, and then incubated with primary antibodies (10–20 μg/ml) for 30 min. After six 5-min washes in PBS, the cells were incubated with Texas red–conjugated secondary antibodies for 30 min. The coverslips were washed 10 times for 5 min with PBS, mounted in Aqua-Poly/Mount (Polyscience, Warrington, PA) and viewed under a fluorescence microscope (Axiophoto; Carl Zeiss, Inc., Thornwood, NY) or an MRC-600 confocal microscope (Bio Rad, Hercules, CA).

Preparation and Immunogold Labeling of "Ripped-off" Plasma Membrane

"Ripped-off" plasma membranes were prepared by the method of Sanan and Anderson (1991). Transformed HtTA cells were cultured on glass coverslips as described above, and were incubated with D65-gold in serum-free medium (SFM) for 60 min at 4°C. Cells were washed briefly and incubated in SFM at 37°C for 3 min. The coverslips were washed twice with PBS and once with KSHM (100 mM KOAc, 85 mM sucrose, 20 mM Hepes, and 1 mM $MgCl_2$, pH 7.4) at 4°C, and were transferred cell-side-down onto poly-L-lysine–treated, Formvar-coated nickel grids that had been placed on cellulose acetate membrane filters. After aspirating excess buffer, rubber stops were gently put on the coverslips, left for 60 s, and then removed. KSHM was added to the edge of each coverslip which was then also removed. EM grids carrying adherent plasma membrane fragments were collected with a forceps and immediately fixed with 4% glutaraldehyde in KSHM for 30 min at 4°C. They were washed with PBS, fixed with 1% osmium tetroxide in PBS for 10 min at room temperature and washed with distilled water three times for 5 min. The grids were incubated with 1% tannic acid in distilled water, washed with distilled water three times for 5 min, and incubated with 1% uranium acetate in distilled water for 10 min. After washing with distilled water three times for 1 min, grids were air dried and viewed with an electron microscope (CM10; Phillips Electronic Instruments Co., Mahwah, NJ) at 80 kV.

For immunostaining, the plasma membrane preparations were more lightly fixed with 4% paraformaldehyde and 1% glutaraldehyde in KSHM for 60 min at 4°C. All the following steps were done at 4°C. The grids were washed 6× 5 min with PBS and quenched with 1 mg/ml sodium borohydrate in PBS for 10 min. The grids were washed three times with PBS, blocked with 1% BSA, 5% normal goat serum, 0.02% sodium azide for 60 min, incubated with hudy-1 (10 μg/ml) for 2 h, washed 10× 5 min with PBS, and then incubated with gold-conjugated secondary antibody for 2 h. After washing 10× 5 min with PBS, the samples were fixed with 4% glutaraldehyde in PBS for 30 min. They were then fixed with 1% osmium tetroxide, processed, and viewed as described above.

For the quantification of ripped-off membrane preparations, negative films taken at ×15,500 were digitized using a Molecular Dynamics personal densitometer. Quantitative analysis on 10–12 negatives per cell type was performed on a Macintosh IIfx computer using the public domain NIH Image program version 1.55 (written by Wayne Rasband, National Institutes of Health, Bethesda, MD, and available from the Internet by anonymous ftp from zippy.nimh.nih.gov or on floppy disk from NTIS, Springfield, VA; No. PB93-504868).

Immunogold Labeling on Ultrathin Cryosections

The induced cells were fixed with 4% paraformaldehyde and 1% glutaraldehyde in 0.1 M phosphate buffer for 30 min at 4°C. Ultrathin cryosections were prepared and immunostained with hudy-1 (20 μg/ml) and colloidal gold conjugated secondary antibody as previously described (Balch et al., 1994).

Negative Staining

Coated vesicles were isolated from a bovine brain extract on sucrose gradients using published procedures (Pearse, 1975). Coated vesicles (100 μg/ml) were adsorbed to Formvar-coated nickel grids for 5 min at room temperature, the grids were washed three times with PBS and fixed with 1% glutaraldehyde in 0.1 M phosphate buffer for 30 min. After washing 5× 5 min with PBS and blocking with 1% BSA in PBS for 60 min, the samples were incubated with hudy-1 (10 μg/ml) in BSA/PBS for 60 min. The grids were washed six times with PBS for 5 min, and they were incubated with colloidal gold conjugated secondary antibody for 5 h. After washing 10× 5 min with PBS, the grids were negatively stained with 2% uranyl acetate in distilled water for 5 min, blotted with filter paper, and air dried.

Other Electron Microscopy Techniques

For conventional Epon sections, the cells were cultured in four-well plates (Nunc, Roskilde, Denmark) in the absence of tet for 48 h. They were fixed with 2.5% glutaraldehyde in 0.1 M phosphate buffer, pH 7.4, for 30 min, postfixed with 1% osmium tetroxide in 0.1 M phosphate buffer, pH 7.4, for 30 min, and processed for embedding in Epon as described (Lamaze et al., 1993). For ruthenium red staining, the cells were fixed with 1.2% glutaraldehyde, 0.5 mg/ml ruthenium red (Ted Pella Inc.) in 66 mM cacodylate buffer, pH 7.2, for 60 min. The cells were washed with 150 mM cacodylate buffer three times for 3 min. They were fixed again with 1.3% osmium tetroxide, 0.5 mg/ml ruthenium red in 33 mM cacodylate buffer for 3 h at room temperature. The cells were washed with 150 mM cacodylate buffer three times for 5 min, and processed for embedding in Epon as above. These samples were observed with Phillips CM10 and Hitachi HU12A electron microscopes at 80 kV and 75 kV.

Results

elel Mutant Dynamin is Impaired in GTP Binding and Hydrolysis

We have previously shown (van der Bliek et al., 1993) that transient overexpression of a dynamin mutant in HeLa cells blocks coated vesicle formation at an intermediate stage after the initiation of coat assembly but preceding the sequestration of ligands into constricted coated pits. The dynamin mutant, designated element 1 (elel) contains a $Lys^{44} \rightarrow Ala$ substitution in the first of three nucleotide-binding elements conserved among all members of the GTPase superfamily. This mutation was predicted to have greatly reduced guanine nucleotide–binding affinity and, therefore, impaired GTPase activity by analogy to other members of the GTPase superfamily (Pai et al., 1990; van der Bliek et al., 1993). To confirm this prediction, recombinant wild-type and elel mutant dynamin were expressed in Sf9 insect cells using the baculovirus expression system and purified to near homogeneity (Warnock, D. E., J. L. Terlecky, and S. L. Schmid, manuscript submitted for publication). GTP hydrolysis by wt and elel dynamin was directly measured, and the results are shown in Fig. 1. Like native bovine brain dynamin, wild-type recombinant human dynamin had low intrinsic GTPase activity that could be stimulated by the addition of microtubules (Fig. 1 *A*) (Shpetner and Vallee, 1992). In contrast, under these conditions, elel mutant dynamin showed no detectable intrinsic or microtubule-stimulated GTPase activity (Fig. 1 *B*). At higher concentrations of GTP (>300 μM), the intrinsic and MT-stimulated GTPase activity of elel dynamin could be detected, suggesting that the defect in GTPase activity was in part caused by decreased affinity for GTP (data not shown). These in vitro data strengthen the argument that the inhibitory effect of the elel mutant on coated vesicle formation observed in transiently transfected cells was caused by its inability to bind and hydrolyze GTP (van der Bliek et al., 1993).

Conditional Expression of Wild-type and Mutant Dynamin in Stably Transformed Cells

Stably transformed cell lines expressing wt and elel dynamin

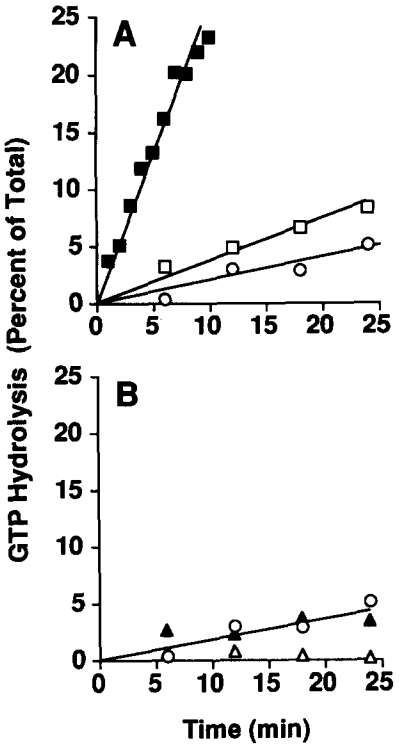

Figure 1. MT-stimulated GTPase activity of recombinant wild-type and elel mutant dynamin. GTP hydrolysis by (*A*) wild-type or (*B*) elel mutant (Lys^{44}→Ala) dynamin purified from recombinant baculovirus-infected Sf9 insect cells was assayed in the presence or absence of microtubules as described in Materials and Methods. Shown are the kinetics of GTP hydrolysis by dynamin alone (□, △), taxol-stabilized microtubules alone (○), or taxol-stabilized microtubules and dynamin together (■, ▲).

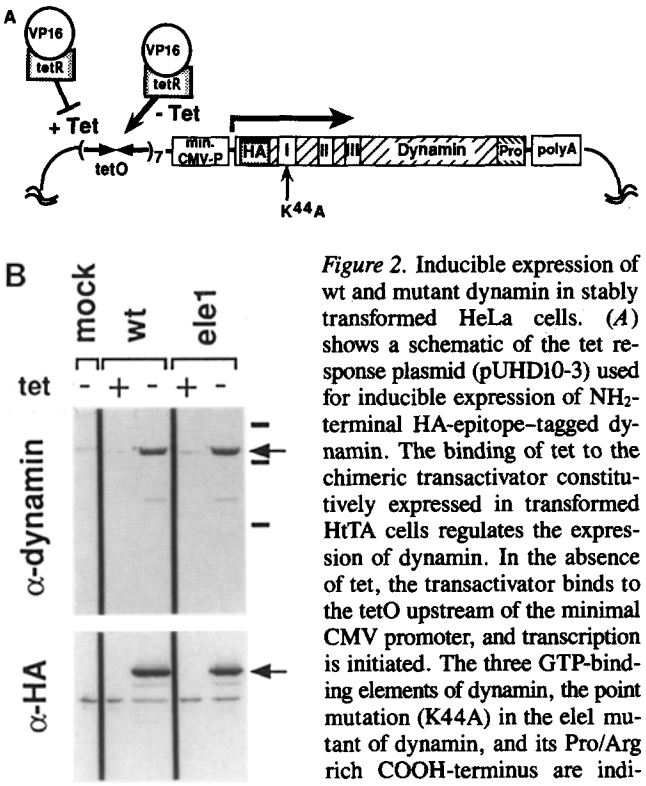

Figure 2. Inducible expression of wt and mutant dynamin in stably transformed HeLa cells. (*A*) shows a schematic of the tet response plasmid (pUHD10-3) used for inducible expression of NH_2-terminal HA-epitope-tagged dynamin. The binding of tet to the chimeric transactivator constitutively expressed in transformed HtTA cells regulates the expression of dynamin. In the absence of tet, the transactivator binds to the tetO upstream of the minimal CMV promoter, and transcription is initiated. The three GTP-binding elements of dynamin, the point mutation (K44A) in the elel mutant of dynamin, and its Pro/Arg rich COOH-terminus are indicated. (*B*) Western blot analysis shows the tight regulation of dynamin expression in the presence of tet and the induction of high levels of dynamin expression after removal of tet. After cultivation in the absence (−) or presence (+) of tet (2 μg/ml) for 48 h mock, wild-type, and elel cells were washed twice with PBS and immediately lysed in Laemmli sample buffer. Lysates corresponding to 50,000 cells per lane were separated on a 7.5% gel and analyzed by Western blot using anti-dynamin or anti-HA antibodies. The arrows indicate dynamin, and the bars indicate the position of the molecular mass markers 116, 97.4, and 66 kD.

were generated to allow a more detailed biochemical and morphological examination of the mutant's effects on cell function. To distinguish recombinant dynamin from endogenous, the cDNA constructs for wild-type and elel mutant dynamin described previously (van der Bliek et al., 1993) were modified by an NH_2-terminal addition of 30 bp encoding 10 amino acids of an HA-tag (MQYDVPDYAH) (Wilson et al., 1984). When tested in transiently transfected cells, the HA-modified wild-type had no phenotype, and we observed similar inhibitory effects on the internalization of transferrin for the elel mutant with or without the HA-tag (data not shown). The dynamin cDNA was subcloned into pUHD10-3 downstream of seven repeat units of the tet-responsive elements from *E. coli* and a minimal cytomegalovirus promoter (see Fig. 2 *A*) (Gossen and Bujard, 1992). This vector allows inducible expression of cDNAs when transfected into HtTA HeLa cells expressing a chimeric transactivator (tTA). tTA is comprised of the tet repressor fused to the COOH-terminal domain of VP16, a viral transcription activator (Gossen and Bujard, 1992). Removal of tet from the media permits binding of tTA to the tet operator (tetO) response elements and efficient transcription (Fig. 2 *A*).

Mutant and wt dynamin cDNA constructs were cotransfected into HtTA cells with the selectable marker for puromycin. After selection and subcloning, positive clones were screened for dynamin expression in the absence of tet. The data in Fig. 2 *B* show that 48 h after removal of tet, there was significant overexpression of both wt and elel recombinant dynamin. Compared with mock-transfected cells in the absence of tet, the overexpression of both recombinant wt and elel dynamin was at least 50-fold over endogenous dynamin when quantitated by Western blot analysis using the monoclonal antibody, hudy-1. Hudy-1 recognizes epitopes that are shared by both neuronal and somatic isoforms of dynamin (Warnock et al., manuscript in preparation) referred to as dynamin-1 and dynamin-2, respectively (Sontag et al., 1994, Cook et al., 1994). Probing Western blots with the anti-HA antibody demonstrated the tight control of gene expression in these stable cell lines as no recombinant dynamin was detectable in cells grown in the presence of tet (Fig. 2 *B*).

Dynamin Is Associated with the Plasma Membrane

Cell fractionation studies have established that dynamin is located both on membrane fractions and in the cytosol (Scaife and Margolis, 1990; Tuma et al., 1993; van der Bliek et al., 1993), suggesting that dynamin may cycle between these two pools. In mock-transformed HtTA cells, endogenous dynamin partitioned equally between soluble and membrane-associated pools. After induction, there was a fivefold

increase in the amount of dynamin present in the particulate fraction, although most of the overexpressed wt and elel dynamin accumulated in the cytosol (data not shown). These data are consistent with our previous results in transiently transfected cells (van der Bliek et al., 1993), and suggested that the accumulation of overexpressed dynamin in the cytosol was due to a limited availability of membrane-associated binding sites.

To examine the specific membrane localization of both endogenous and overexpressed HA-tagged dynamin, cells were gently permeabilized with digitonin and washed to deplete soluble proteins before fixation and staining. Fig. 3 shows confocal immunofluorescence images of dynamin detected with the anti-dynamin mAb, hudy-1 (Fig. 3, *A*, *C*, and *E*), which detects both endogenous and overexpressed HA-tagged dynamin (Warnock, D. E., J. L. Terlecky, and S. L. Schmid, manuscript submitted for publication) and with the anti-HA-tag mAb 12CA5 (Fig. 3, *B*, *D*, and *F*) after inducing expression by removal of tet. Each sample was costained with the anti-clathrin IgM mAb CHC5.9 (Fig. 3, *A'-F'*). Staining of endogenous dynamin in mock-transfected cells with hudy-1 revealed a punctate pattern that significantly overlapped with clathrin staining (compare Fig. 3, *A* and *A'*). As expected from Western blot analysis, there was no detectable staining of mock cells using the anti-HA mAb (Fig. 3 *B*), nor of wt or elel cells grown in the presence of tet (not shown). Removal of tet from the media induced expression of recombinant dynamin in both wt and elel cells, which was detected as a dramatic increase in staining by the anti-HA mAb (Fig. 3, *D* and *F*). Staining of total membrane associated dynamin using hudy-1 revealed a less dramatic increase (Fig. 3, *A* vs. *C* and *E*) consistent with the existence of a saturable membrane-binding site. Membrane-associated wild-type and mutant dynamin continued to show plasma membrane staining patterns that overlapped considerably with the clathrin staining pattern (Fig. 3 *C'-F'*).

Plasma Membrane-associated Dynamin is Specifically Localized to Clathrin-coated Pits

Ultrastructural studies were performed to more precisely examine the localization of endogenous and overexpressed dynamin relative to coated pits at the cell surface. For this purpose, EM grids were applied to the upper surface of the cells and then peeled off, bringing large areas of plasma membrane with them. These were subsequently fixed and stained to visualize the polygonal clathrin lattices on the cytoplasmic surface of these ripped-off plasma membranes (Sanan and Anderson, 1991). The micrographs in Fig. 4 *a-e* show the cytoplasmic surface of plasma membranes from mock-transfected HtTA cells (Fig. 4, *a* and *b*), as well as from HtTA cells overexpressing wild-type (Fig. 4 *c*) and elel (Fig. 4, *d* and *e*) dynamin, which have been immunostained with antidynamin, followed by detection with gold-conjugated secondary antibodies. Gold particles detecting endogenous dynamin (Fig. 4, *a* and *b*) were rarely detected on uncoated plasma membrane surfaces and, instead, were almost exclusively located in clathrin-coated pits. Both flat clathrin lattices (*open arrows*) and highly curved clathrin lattices (*arrowheads*) were labeled. No labeling was detected with secondary antibody only (not shown). The labeling pattern of endogenous dynamin on these structures was diffuse without any preference to the neck region of the even highly curved coated pits. This selective localization of dynamin to coated pits was true, not only in mock-transfected cells, but also in cells overexpressing both wild-type (Fig. 4 *c*) and elel mutant (Fig. 4, *d* and *e*) dynamin. The finding that dynamin was exclusively associated with coated surfaces, even when overexpressed, suggested that it must be specifically targeted to these structures after clathrin assembly.

Since dynamin was localized to both flat and deeply invaginated coated pits, we next determined whether dynamin remained associated with these structures after coated vesicle budding. The electron micrographs in Fig. 4, *f* and *f'* show a negatively stained preparation of bovine brain coated vesicles that have been immunolabeled with anti-dynamin antibody. Quantitation of these data demonstrated that 70% of coated vesicles (112 of 163 counted) were labeled with 1-6 gold particles. Control specimens in which the primary antibody was omitted showed no labeling (not shown), nor was significant staining observed on contaminating smooth vesicles (~6% of contaminating smooth vesicles were labeled with 1 gold particle, while 93% [92 out of 99 counted] had no label). These results suggest that some portion of dynamin remains associated with clathrin-coated vesicles after budding from the plasma membrane.

To establish the specificity of targeting of endogenous and overexpressed dynamin to plasma membrane-associated coated pits, cryo-ultrathin sections were prepared from fixed HtTA cells and immunostained with hudy-1. Electron micrographs from these experiments are shown in Fig. 5. Consistent with the localization on ripped-off plasma membranes, endogenous dynamin in mock-transfected cells (Fig. 5 *A*), was localized to both flat coated areas (*arrows*) and deep coated pits/vesicles at the plasma membrane (*arrowhead*). Strikingly, even in HtTA cells overexpressing wt (Fig. 5 *B*) and elel mutant (Fig. 5 *C* and *D*) dynamin, only coated structures on or near the plasma membranes were labeled. For both mock- and dynamin-transfected cells, almost no labeling was observed outside of coated structures on the plasma membranes. As expected from the immunofluorescence studies, there was a marked increase in cytosolic staining in cells overexpressing both mutant and wt dynamin. Slight staining observed in the area of the *trans*-Golgi network was not significantly higher than the diffuse cytosolic staining. No labeling was detected in the Golgi complex (*Gc*), the mitochondria (*m*), or the nucleus (*n*). These results, together with the immunolocalization on ripped-off membranes, demonstrated that dynamin was specifically targeted to coated pits at the plasma membranes of HtTA cells.

Expression of Mutant Dynamin Inhibits Receptor-mediated Endocytosis of Transferrin and EGF

While it has previously been demonstrated that transient overexpression of mutant dynamin in mammalian cells blocks receptor-mediated endocytosis of Tfn (van der Bliek et al., 1993; Herskovits et al., 1993*a*), these systems did not allow for an accurate quantitative assessment of the effect of dynamin mutants on endocytosis. Nor did they allow investigation of the specificity of the observed effects. With the availability of homogeneous, stably transformed cell lines expressing equivalent amounts of either wt or elel mutant dynamin, these issues can now be addressed.

Receptor-mediated endocytosis of BSST in stably trans-

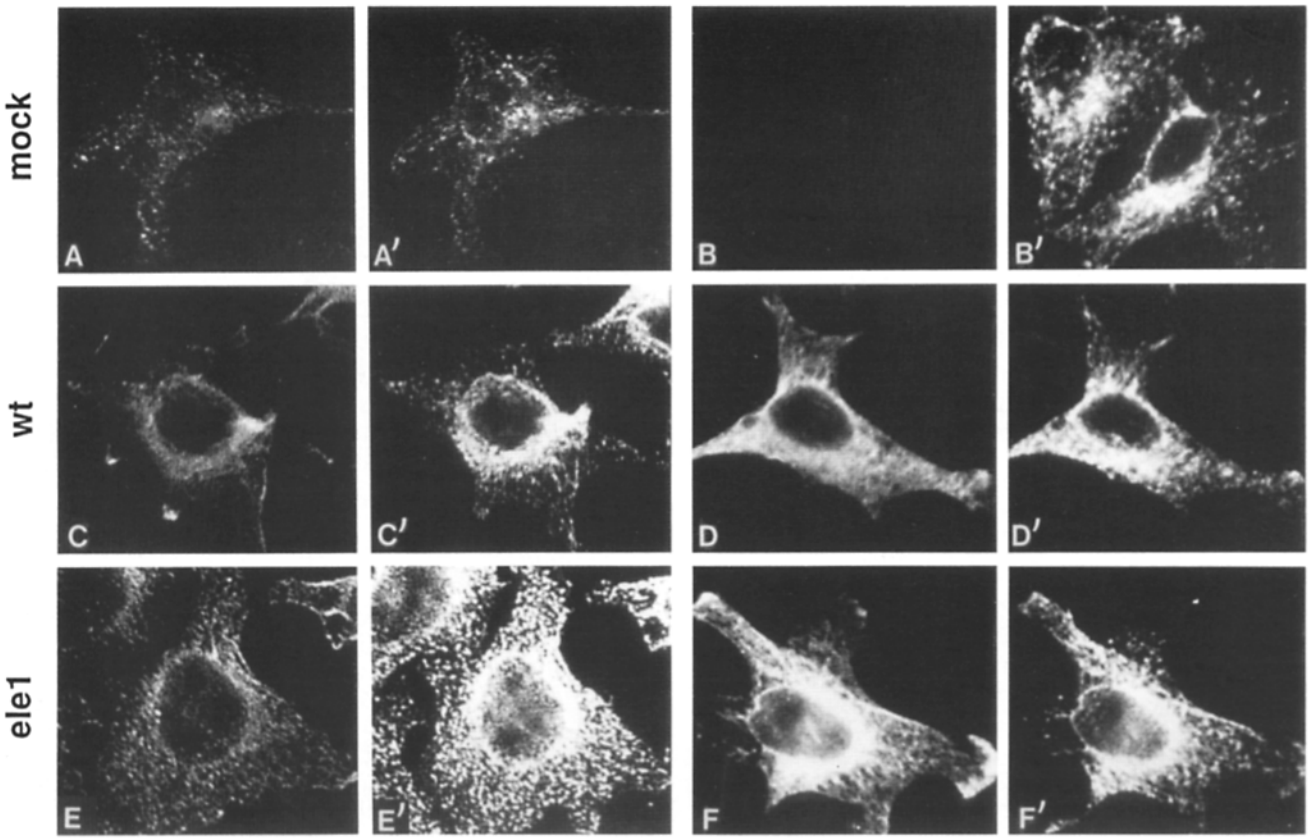

Figure 3. Double immunofluorescence labeling of endogenous or overexpressed dynamin and clathrin. After 48 h of induction in the absence of tet, mock (*top row*), wt (*middle row*), and elel (*bottom row*), HtTA HeLa cells were permeabilized with digitonin, washed briefly, fixed, and processed for indirect immunofluorescence using anti-dynamin (*A*, *C*, and *E*), anti-HA (*B*, *D*, and *F*), or anti-clathrin (*A'–F'*) mAbs. The secondary antibodies were FITC-conjugated goat anti-mouse IgG (γ chain specific) for dynamin and HA, and Texas red–conjugated goat anti-mouse IgM (μ chain specific) for clathrin.

formed cells was measured by its acquired inaccessibility to exogenously added avidin. In addition to detecting the internalization of biotinylated ligands into sealed, coated vesicles, this assay also detects the formation of a potential intermediate in which receptor-bound ligands are sequestered into constricted coated pits (Schmid and Carter, 1990; Carter et al., 1993; van der Bliek et al., 1993). The data in Fig. 6 *A* show that overexpression of wt dynamin did not affect the initial rate of sequestration of Tfn as compared to mock-transfected cells. Similarly, Tfn endocytosis in uninduced wt and elel cells was indistinguishable from mock-transfected cells grown in either the presence or absence of tet (not shown). In contrast, overexpression of elel dynamin cells inhibited the initial rate of sequestration of Tfn into either constricted coated pits or coated vesicles by >80%.

Transferrin receptors are constitutively internalized via clathrin-coated vesicles. To confirm the general effect of overexpression of elel dynamin on receptor-mediated endocytosis, we examined the ligand-induced endocytosis of EGF-R in wt and elel cells. Endocytosis of EGF via clathrin-coated vesicles was followed using BEGF and quantified by its acquired inaccessibility to avidin as previously described (Lamaze et al., 1993). As shown in Fig. 6 *B*, the internalization of BEGF was also inhibited (>60%) in cells expressing elel mutant dynamin as compared to wt or mock-transformed cells. The uptake of EGF was generally less efficient than the uptake of transferrin; however, for both ligands, endocytosis in elel cells was reduced to a similar residual rate (~2.5%/min; Fig. 5 *B*). Together with the data on Tfn uptake, these results support our previous conclusion (van der Bliek et al., 1993) that overexpression of the elel mutant of dynamin blocks the sequestration of receptor-bound ligands into constricted coated pits.

Coated Pit Structures Accumulate on the Plasma Membrane of Dynamin Mutant Cells

The observed defect in ligand sequestration into constricted coated pits could be caused by either a block in the mechanics of coated vesicle formation, as previously proposed (van der Bliek et al., 1993), or by a defect in recruiting receptors into coated pits through recognition of "internalization motifs" in their cytoplasmic domains (Trowbridge et al., 1993). We, therefore, directly examined the nature of the intermediates that accumulate in the mutant cells at the ultrastructural level. For these studies, cells were incubated in the presence of gold-conjugated D65 anti-human Tfn-R mAbs (D65-gold) at 4°C for 60 min, and were then warmed briefly (3 min) at 37°C to label surface Tfn-R. Ripped-off plasma membranes were prepared, fixed, and stained to allow simultaneous visualization of the surface-bound D65-gold and the cytoplasmic surface of the plasma membrane (Sanan and Anderson, 1991).

Electron micrographs of representative areas of the cyto-

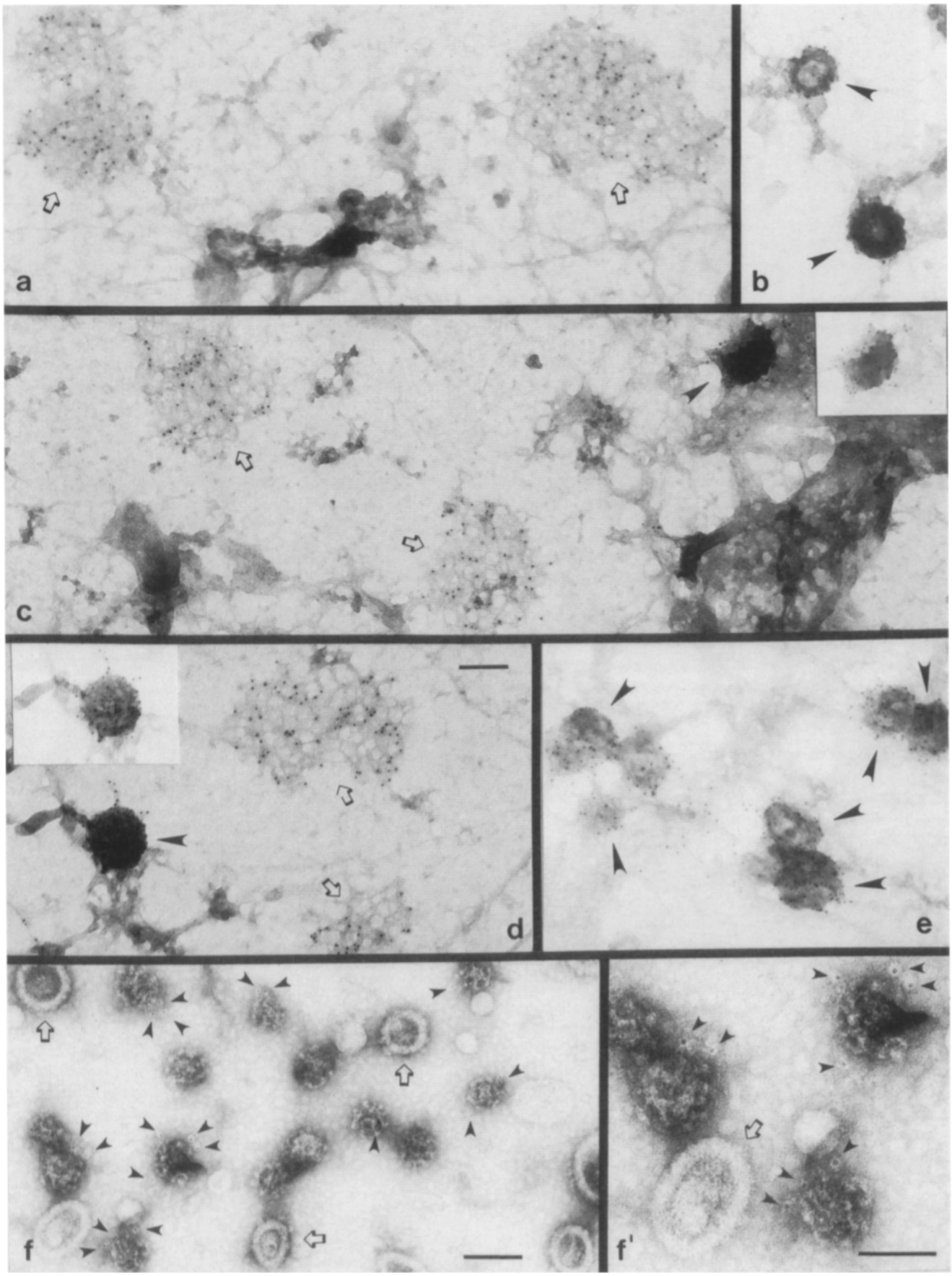
a
b
c
d
e
f
f'

plasmic plasma membrane surface from induced wt and elel cells are shown in Fig. 7. Flat and curved clathrin lattices are indicated in the figure by open arrows and arrowheads, respectively. While there was little qualitative difference between mock cells (not shown) and wt cells, the cytoplasmic surface of the plasma membrane in elel cells showed a dramatic increase in the number of curved clathrin lattices representing invaginated coated pits, often appearing in clusters. Quantitation of these results (Table I *A*) revealed an approximately twofold increase in the number of curved clathrin lattices per square micrometer of membrane in elel cells and a corresponding approximately twofold decrease in the number of flat clathrin lattices, as compared to wt or mock cells. These results suggest that overexpression of elel dynamin resulted in an accumulation of invaginated coated pits at the expense of flat clathrin lattices. The average area of the remaining flat lattices was also reduced in the elel cells. In contrast, the average area of curved coated pits was apparently unaltered, suggesting at this level of resolution that the coated pit intermediates that accumulate in elel cells were structurally similar to intermediates found normally in wt cells. The twofold increase observed in the number of invaginated coated pits was consistent with an almost complete block in coated vesicle budding since this accumulation was probably limited by the cytoplasmic pool of coat components (see below). From these data, we conclude that in cells overexpressing elel dynamin, invaginated coated pits fail to become constricted and to pinch off, thereby resulting in their accumulation and the observed inhibition of receptor-mediated endocytosis.

Transferrin Receptors Are Efficiently Sorted into Coated Pits in Dynamin Mutant Cells

Constricted coated pits can be distinguished biochemically from invaginated coated pits by their ability to sequester receptor-bound, biotinylated ligands from exogenously added avidin. However, the ultrastructural techniques described here do not allow these intermediates to be distinguished morphologically. Therefore, the possibility that mutant dynamin affects the sorting of receptors into coated pits remained viable. This possibility was especially intriguing since dynamin is related to the SRP54 GTPase, which recognizes signal sequences on nascent polypeptides and recruits them to ER membranes (Gilmore, 1991). However, quantitative evaluation of the sorting efficiency for Tfn-R in coated pits in mock, wt, and elel cells (Table I *B*) revealed no significant differences. While the number of Tfn-R (D65-gold particles) per square micrometer of cell surface in elel mutant cells was at least twofold higher than that observed for mock or wt cells, the concentration of Tfn-R in coated pits (calculated as the ratio of the number of D65-gold particles per square micrometer of coated membrane to the number of D65-gold particles per square micrometer of smooth membrane) was not significantly affected (23.6-fold concentration in wt cells compared to 18.5-fold for elel mutant cells). These numbers suggest that the sorting efficiency for transferrin receptors into coated pits was the same for wt and elel mutant cells and, therefore, that overexpression of dynamin mutants defective in GTP binding and hydrolysis does not interfere with efficient recruitment of receptors into coated pits. Since receptor recruitment into coated pits and coat assembly are apparently unaffected, these early events in coated vesicle formation can be excluded as targets for the function of dynamin's GTPase.

Recycling of Transferrin Receptors to the Plasma Membrane is Unaffected in elel Cells

So far, we have provided strong evidence that mutant dynamin blocks the constriction and budding of coated pits to form coated vesicles at the cell surface. As vesicle budding is a common requisite to all membrane traffic events, we tested whether overexpression of elel dynamin affected any other intracellular transport pathway. The approximately twofold increase in Tfn-R expression at the plasma membrane in elel cells observed by EM (Table 1 *B*) and by total binding of BSST to the cell surface in elel mutant cells at 4°C (data not shown) could reflect either continued recycling of Tfn-R from the endosomal compartment to the plasma membrane or increases in total expression of Tfn-R. We, therefore, examined the steady-state distribution of transferrin receptors in mock, wt, and elel cells by determining what fraction of the total Tfn-R were accessible to proteolytic digestion by trypsin at 4°C. Quantitative analysis showed that the fraction of Tfn-R found on the surface of cells overexpressing wt dynamin (20.9 ± 6.6%, n=5) was the same as that found in mock-transformed cells (22.9 ± 3.4%, n=2). In contrast, there was more than a twofold increase in the fraction of Tfn-R distributed on the cell surface of elel cells (51.2 ± 10.6%, n=5). The intracellular: surface distribution of Tfn-R reflects the relative rates of internalization and recycling (Ciechanover et al., 1983). Thus, the extent of redistribution of Tfn-R to the cell surface (from an 80:20 distribution to a 50:50 distribution) is consistent with the observed fivefold decrease in internalization rates and an unaltered rate of recycling. To confirm this, we directly measured the rate of Tfn recycling in wt cells and cells expressing elel dynamin. Cells were labeled to equilibrium with B-Tfn, and surface Tfn was masked with avidin. The data in Fig. 8 *A* show the kinetics of loss of intracellular biotinylated Tfn as the cells were reincubated for increasing times at 37°C.

Figure 4. Dynamin is associated with coated pits and coated vesicles. After 48 h of induction, ripped-off membranes were prepared from mock (*a* and *b*), wt (*c*), and elel (*d* and *e*) cells, fixed, and processed as described in Materials and Methods. Samples were immunostained with anti-dynamin mAb and goat anti-mouse IgG conjugated to colloidal gold (5 nm). Open arrows indicate planar clathrin lattices, and arrowheads indicate curved clathrin lattices. Insets show underexposed images to identify gold particles. Bar, 0.1 μm. (*f*) Coated vesicles from bovine brain cytosol that were adsorbed to poly-L-lysine–treated, Formvar-coated nickel grids, fixed, and immunostained with hudy-1 mAb, and goat anti-mouse IgG coupled to colloidal gold (5 nm). The grids were observed after negative stain with uranyl acetate. Arrowheads show gold particles on coated vesicles. Open arrows show contaminating noncoated membranes. Bar, 0.1 μm. (*f'*) Enlarged region of the bottom left corner of *f*. Bar, 50 nm.

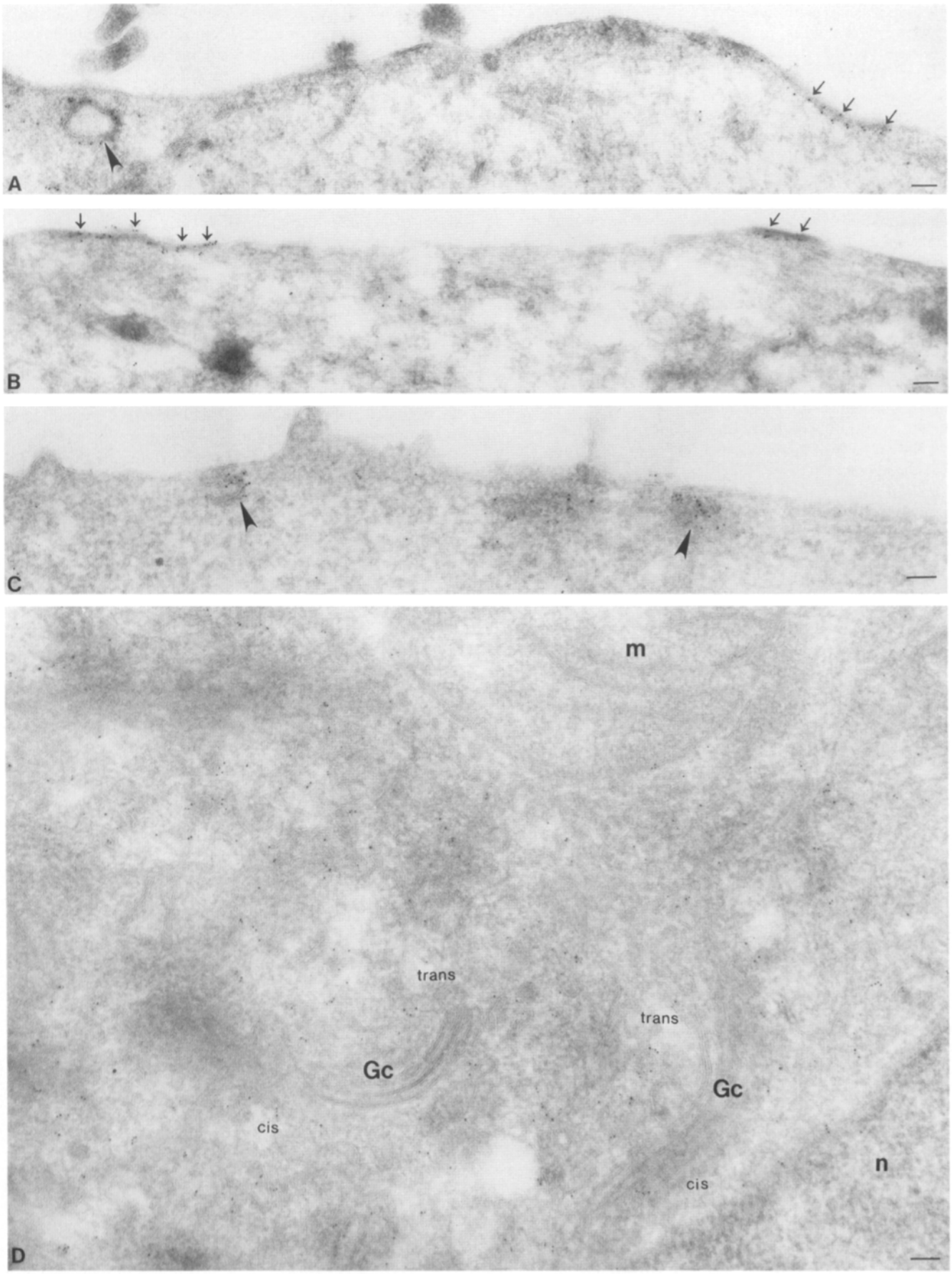

Figure 5. Cryo-immunoelectron microscopy of dynamin on ultra-thin sections. After 48 h of induction, mock (*A*), wt (*B*), and elel (*C* and *D*) HeLa cells were fixed and processed for cryo-ultrathin section as described in Materials and Methods. Dynamin was immunolocalized with hudy-1 mAb and anti-mouse IgG conjugated to colloidal gold (5 nm). Small arrows indicate flat coated surfaces, and arrowheads indicate curved coated surfaces. Mitochondria (*m*), Golgi complexes (*Gc*), and the nucleus (*n*) are indicated. Bar, 0.1 μm.

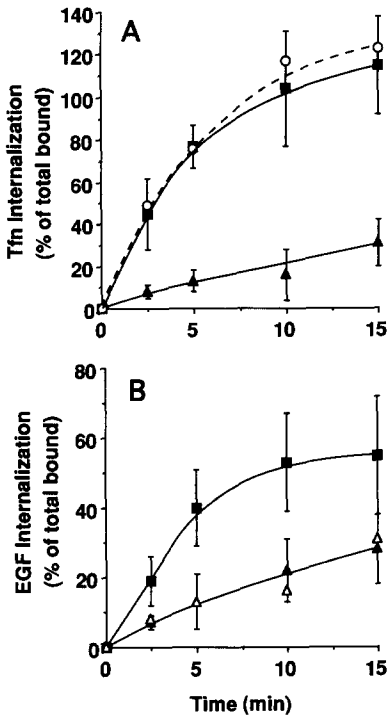

Figure 6. Receptor-mediated endocytosis of transferrin and EGF is inhibited in the dynamin mutant. After 48 h of induction in the absence of tet, the internalization of transferrin (*A*) or EGF (*B*) was followed in cells expressing either wild-type (■) dynamin, elel mutant dynamin (▲), or in mock-transformed cells (○). For comparison, the residual rate of transferrin uptake in elel cells in *A* is shown in *B* (△). After incubation for the indicated times at 32°C, the amount of internalized BSST or BEGF was quantified by avidin accessibility as described.

As can be seen, Tfn is recycled from wt and elel cells with identical kinetics ($t_{1/2}$ ~7–8 min).

Mutant Dynamin Does not Affect TGN-derived Coated Vesicle Function

We next examined whether overexpression of elel dynamin affects intracellular trafficking events along the biosynthetic pathway by following the transport of newly synthesized transferrin receptor from the ER, through the Golgi, and to the cell surface. For these experiments, cells were pulse-labeled with [^{35}S]methionine for 15 min and then chased for ≤4 h before precipitation of metabolically labeled Tfn-R and analysis by SDS-PAGE, as described in Materials and Methods. In three independent experiments (data not shown), we found no differences between elel and wt cells in the rate of transport of Tfn-R from the ER to the medial Golgi (as judged by the acquisition of endoH resistance), through the Golgi to the *trans*-Golgi network (TGN) (as judged by the electrophoretic mobility shift upon addition of complex oligosaccharides) or to the cell surface (as monitored by tryptic digest of receptors at the cell surface). These results suggest that overexpression of elel mutant dynamin does not affect transport by COP- or other coated vesicles along the biosynthetic pathway.

To address the question of whether the budding of Golgi-associated, clathrin-coated vesicles is affected in cells overexpressing the dynamin mutant, we followed the biosynthesis of a lysosomal enzyme, cathepsin D. Mannose-6-phosphate-containing lysosomal enzymes are sorted at the level of the TGN by binding to mannose-6-phosphate receptors that are concentrated in clathrin coated pits (reviewed by Kornfeld and Mellman, 1989). In HtTA cells, cathepsin D exists as a 49-M_r precursor in the Golgi apparatus, and it is delivered via clathrin-coated vesicles from the TGN to an endosomal compartment where it is processed to a 46-M_r form. Delivery to lysosomes results in further processing to a 32-M_r mature form (Gieselmann et al., 1983). Metabolically labeled cathepsin D was immunoprecipitated after various chase times from wt and elel cell lysates using a polyclonal serum (Gieselmann et al., 1983). The appearance in the lysosomes of the 32-kD mature form of cathepsin D was detected by SDS-PAGE and quantified by phosphorimager analysis as described in Materials and Methods. The data in Fig. 8 *B* show quantitation of results from one representative experiment. The 32-kD mature form of cathepsin D was first detected in cells expressing elel dynamin after 57 ± 8 min of chase (n = 3), unchanged from when it was first detected in wt cells (59 ± 6 min of chase; n = 3). These results demonstrate that overexpression of elel dynamin did not affect

Table I. Quantitation of the Accumulation of Coated Pits on the Plasma Membrane of HeLa Cells Expressing Mutant Dynamin

A. Cell line	Total area measured	No. of flat lattices	Avg. area of flat lattices	No. of curved lattices	Avg. area of curved lattices
	μm²	*per 10 μm²*	*μm²*	*per 10 μm²*	*μm²*
mock	252	3.8	0.27 ± 0.18	2.2	0.010 ± .005
wt	162	2.6	0.35 ± 0.25	2.3	0.011 ± .006
elel	238	1.5	0.20 ± 0.13	4.9	0.011 ± .007

B. Cell line	Tfn-R/μm² total membrane	Tfn-R/μm² smooth membrane (*A*)	Tfn-R/μm² coated membrane (*B*)	Fold concentration of Tfn-R in coated pits (*B/A*)
mock	22.1	16.4	462	28.2
wt	13.7	10.8	255	23.6
elel	40.8	37.3	691	18.5

Negatives of electron micrographs were prepared as described in Fig. 5. (*A*) Quantitation of the number and area of flat and curved clathrin lattices on plasma membrane preparations from mock, wt, and elel HeLa cells. (*B*) Quantitation of the number of anti-Tfn-R-D65-gold particles per square micrometer of total, smooth, or coated plasma membrane. The fold concentration of Tfn-R in coated pits was estimated as the ratio of the number of D65-gold particles per square micrometer of coated membrane to the number of D65-gold particles per square micrometer of smooth membrane.

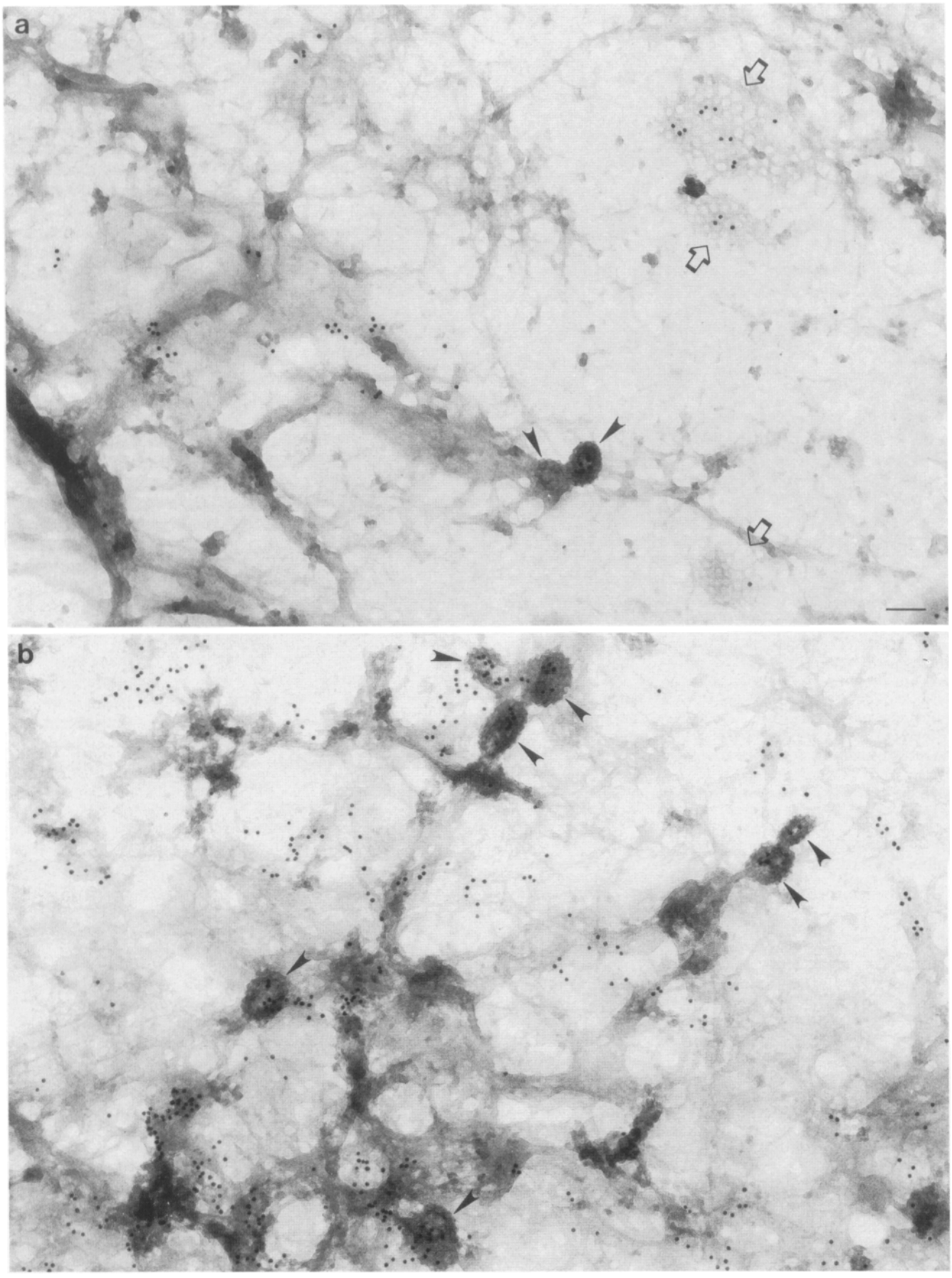
a
b

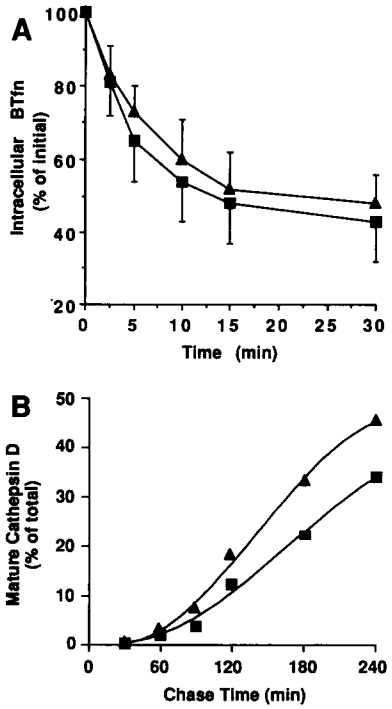

Figure 8. Tfn-R recycling and sorting to lysosomes are not affected by the overexpression of mutant dynamin. (*A*) Cells were incubated for 60 min with B-Tfn at 37°C, removed to ice, and surface-bound B-Tfn was quenched with avidin. The cells were returned to 37°C and incubated for the indicated times in the presence of excess unmodified Tfn. The amount of cell associated B-Tfn that remained inaccessible to a second incubation with avidin was then determined. Data shown are averages ± SD (n = 7). (*B*) HeLa cells stably transformed with wt dynamin and elel dynamin were pulse-labeled for 30 min with Trans[^{35}S]methionine and chased in complete medium for the indicated times. Cathepsin D was immunoprecipitated, subjected to SDS-PAGE, and quantified by phosphorimager analysis. The kinetics of appearance of the mature form of cathespin D in wt (■) and elel (▲) HtTA cells is shown.

the efficiency of clathrin-coated vesicle sorting and transport from the TGN.

AP2 Molecules Are Specifically Distributed to the Membrane in Dynamin Mutant Cells

Further confirmation that overexpression of elel dynamin specifically affects plasma membrane–associated coated pits was obtained by examining the redistribution of coat protein components from the cytosol to the membrane. We have shown that coated pits accumulate at the cell surface in elel cells. Since the assembly of coated pits at the plasma membrane requires AP2 complexes (Robinson, 1992), we would expect this accumulation in coated pits to result in a corresponding redistribution of AP2 complexes from the cytosolic pool to the membrane. In contrast, coated pits at the TGN require AP1 complexes for their assembly (Robinson, 1992). To determine the extent of AP2 redistribution in elel cells and to examine whether AP1 distribution is similarly affected, we fractionated induced mock, wt, and elel cells into particulate and soluble pools. The AP distributions in these fractions were analyzed by Western blot using the monoclonal antibody 100/1 (Ahle et al., 1988), which detects common epitopes in the β and β' adaptin subunits of AP2 and AP1 complexes, respectively. The data in Fig. 9 show that AP2 and AP1 complexes are distributed approximately equally between the particulate and soluble pools in both mock-transformed and wt cells. In contrast, the β subunits of AP2 complexes are almost quantitatively depleted from the cytosolic fraction in elel mutant cells with a corresponding increase in its appearance in the particulate fraction. Importantly, the amount of the β' subunit of AP1 complexes in the soluble pools is unchanged in the elel cells. These results provide additional evidence that dynamin is specifically involved in the formation of clathrin-coated vesicles at the plasma membrane.

Fluid-phase Uptake Continues in Cells Expressing Mutant Dynamin

Even though receptor-mediated endocytosis is dramatically reduced in elel mutant cells, they remain viable after induction by removal of tet for more than 4 d. This observation strongly suggested that some alternate endocytic pathway continued so as to guarantee the cells' supply of important nutrients, as well as to maintain the balance of cell surface area. Alternative, clathrin-independent pathways of endocytosis have been described (van Deurs et al., 1989) and can be measured by the uptake of bulk fluid-phase markers such as HRP. As shown in Fig. 10, fluid phase uptake of HRP continues in elel cells. The initial rate of fluid phase uptake is apparently unaffected compared to wt cells. The slightly reduced uptake of HRP seen only at later time points is, in general, interpreted as a consequence of changes in the accumulation of HRP in the endosomal compartment (see for example Besterman et al., 1981; Griffiths et al., 1989). These differences in the endosomal accumulation of fluid-phase markers could reflect structural changes within the endosomal compartment resulting from the block in coated vesicle budding, as has been described in nephrocytes from *shibire* flies (Koenig and Ikeda, 1990).

Intracellular Accumulation of Endocytic Membranes in Cells Overexpressing Mutant Dynamin

The biochemical analysis of the phenotype of elel cells has thus far allowed us to conclude that mutant dynamin selectively interferes with coated vesicle formation at the cell surface while not interfering with other membrane trafficking pathways. We next examined the general morphology of mock-transfected cells and cells overexpressing wt dynamin or elel mutant dynamin for two reasons: first, to look for evi-

Figure 7. Clathrin-coated pit structures accumulate at the plasma membrane of the dynamin mutant. Ripped-off plasma membranes were prepared from wt (*a*); and elel (*b*) HtTA cells preincubated with D65-gold as described in Materials and Methods. Both flat clathrin lattices (*open arrows*) and curved clathrin lattices (*arrowheads*) were labeled with D65-gold. In elel cells, clusters of curved lattices were often observed, and there was an increase in the number of D65-gold particles associated with the cell surface. Quantitation of these results is given in Table I. Bar, 0.1 μm.

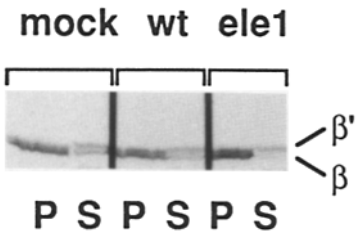

Figure 9. Depletion of AP2, but not AP1 molecules, from the cytosol in mutant dynamin cells. Induced mock, wt, and ele1 cells were lysed by a freeze/thaw step and separated into particulate (*P*) and soluble (*S*) fractions as described in van der Bliek et al. (1993). The subcellular distribution of β/β' adaptins (indicated on the right) was examined by Western blot analysis using the 100/1 anti-β/β' mAb at 3 μg/ml.

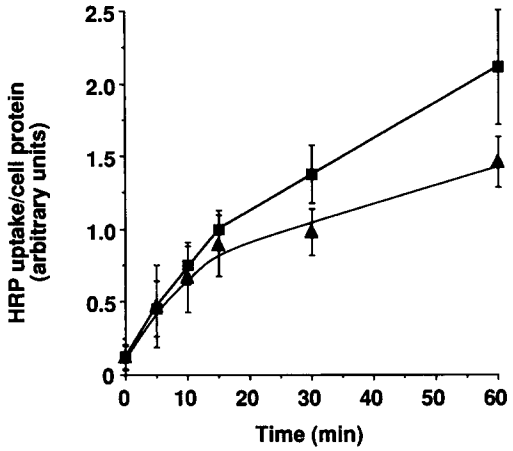

Figure 10. Fluid-phase endocytosis in ele1 cells continues. wt (■) and ele1 (▲) cells were incubated with 1 mg/ml horseradish peroxidase for ≤ 60 min at 32°C and then returned to ice. To determine intracellular HRP, extracellular HRP was digested with 0.1% pronase for 10 min at 4°C. The cells were then extensively washed, pelleted through a sucrose cushion, and cell lysates were prepared as described in Materials and Methods. Cell-associated HRP was photometrically quantified after enzymatic reaction of peroxidase with *o*-phenylenediamine, and was expressed relative to cell protein, determined from aliquots of the same cell lysate.

dence of other cellular functions that might directly or indirectly be perturbed in cells overexpressing mutant dynamin; and second, to directly compare the phenotype of overexpression of ele1 dynamin with that reported for cells expressing the *shibire* mutation so as to better understand the functional relationship of these two homologues.

The electron micrographs in Fig. 11 show ultrathin sections of HtTA cells overexpressing either wt (Fig. 11 *A*) or ele1 mutant dynamin (Fig. 11 *B*) 48 h after culture in the absence of tet. Overexpression of wild-type dynamin had no effect on the general morphology of HtTA cells. However, in cells overexpressing ele1 dynamin, elongated tubular structures (*open arrows*) and numerous structures resembling multivesicular bodies (*arrows*) accumulated in the cytoplasm. Coated structures (*arrowheads*) were closely associated with many of these tubular elements. No alteration in the structure of the Golgi complex (*Gc*) in wt or ele1 cells was detected. Since coated pits were rarely detected on the plasma membrane in thin sections from either wt or ele1 cells, their accumulation could only be measured by sampling larger surface areas using ripped-off membrane preparations (see Fig. 7).

The origin of the membrane tubules that accumulated in cells overexpressing mutant dynamin was explored by incubating cells after fixation with the small, membrane-impermeant electron dense marker, ruthenium red. Only small membrane invaginations connected to the cell surface were typically seen in mock-transfected cells (Fig. 11 *C*) or in cells expressing wt dynamin (Fig. 11 *D*). In contrast, many of the long tubular membranes that specifically accumulated in cells overexpressing mutant dynamin were open to the cell surface and remained accessible to ruthenium red (Fig. 11 *E–G*). These structures were similar to those observed in tissues from *shibire* flies after shift to the nonpermissive temperature (Kosaka and Ikeda, 1993*b*).

Cell Shape and Cytoskeletal Changes Associated with Overexpression of Mutant Dynamin

One of the most striking morphological changes after induction of mutant dynamin could be observed at the light microscopic level as an alteration in cell shape and size. Cells overexpressing wt dynamin showed the same polygonal shape with sharp surface edges (Fig. 12, *a*, *c*, *e* and *e'*) as mock-transfected cells or uninduced HtTA cells cultured in the presence of tet (data not shown). In contrast, as early as 24 h after induction, cells overexpressing ele1 mutant dynamin became large, flattened, and round-edged cells with extended cytoplasm (Fig. 12, *b*, *d*, *f* and *f'*). This striking alteration in cell shape led us to examine the distribution of cytoskeleton and adhesion-related proteins by indirect immunofluorescence. Neither the distribution of microtubules stained with anti-tubulin antibodies (Fig. 12, *a* and *b*) nor of intermediate filaments stained with vimentin (data not shown) were altered in cells overexpressing mutant dynamin. However, there was a striking rearrangement of the actin cytoskeleton, as detected by rhodamine-phalloidin. The stress fibers typically distributed along the entire cell length as seen in wt cells (Fig. 12 *c*) were redistributed from the central cytoplasm to the periphery of ele1 cells (Fig. 12 *d*).

The surface area of ele1 cells attached to the culture substrate appeared dramatically increased over that seen for

Figure 11. Transmission electron microscopy of transformed HtTA HeLa cells. Epon sections vertical to the substrate were prepared from (*A*) wt and (*B*) ele1 cells. Long tubular structures (*open arrows*), many of which have coated ends (*arrowheads*) and structures resembling multivesicular bodies (*closed arrows*), accumulate in ele1 cells. *Gc*, Golgi complex. Bar, 0.2 μm. (*C–G*) HtTA cells were fixed and stained with ruthenium red before preparation of Epon sections as described in Materials and Methods. (*C*) Mock-transfected cells and (*D*) cells overexpressing wt dynamin show few and only short membrane invaginations connected to the cell surface (*small arrows*). (*E–G*) long tubular invaginations (*small arrows*) that are stained with ruthenium red indicating connections to the cell surface in ele1 HtTA cells. Open arrowheads show electron-dense "coats" often present at the ends of these tubular connections. Bar, 0.2 μm.

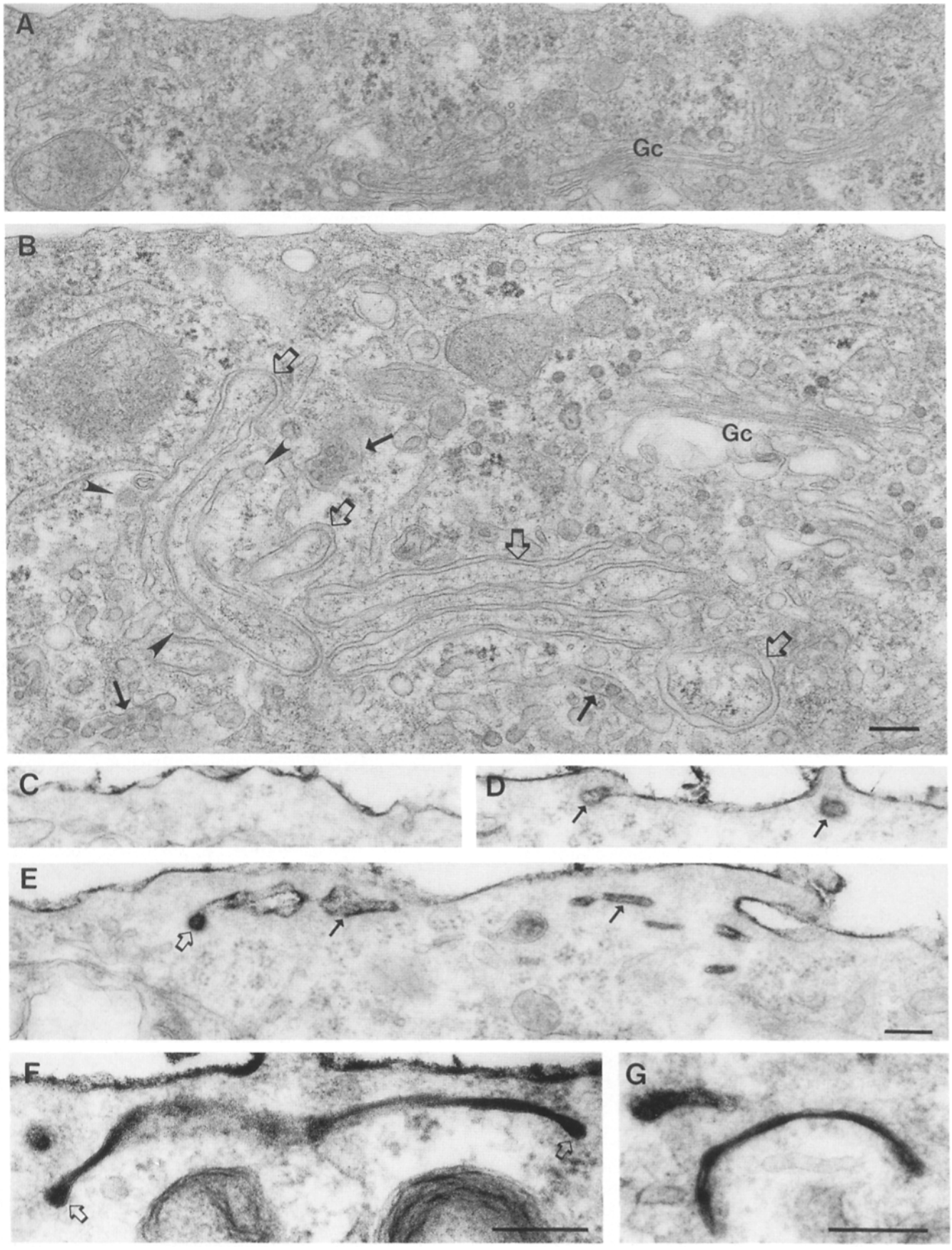
A
Gc
B
Gc
C
D
E
F
G

mock or wt cells. We also observed that elel cells were more resistant to release from the substratum by PBS/EDTA treatment at room temperature (data not shown), suggesting an alteration in cell adhesion properties. The distribution of adhesion plaques in wt and elel-transformed cells was, therefore, examined using anti-vinculin antibodies. Vinculin staining in wt cells was seen in large adhesion plaques (Fig. 12, *e*), which by phase contrast were located at the ends of cell extensions (Fig. 12 *e'*). This staining was indistinguishable from mock-transfected cells (not shown). In contrast, vinculin-staining in elel-transformed cells was detected in somewhat smaller plaques (Fig. 12 *f*) that were uniformly distributed around the entire cell boundary (Fig. 12, *f'*). These results suggest that other cellular functions may be altered either directly or indirectly as a consequence of overexpression of mutant dynamin and inhibition of clathrin-dependent endocytosis.

Discussion

A Dynamin Mutant Potently Blocks Coated Pit Constriction

We have extended previous findings (van der Bliek et al., 1993; Herskovits et al., 1993*a*) that overexpression of a dynamin mutant defective in GTP binding and hydrolysis potently inhibits receptor-mediated endocytosis. Our findings demonstrate that both constitutive and ligand-induced internalization of receptors are affected. Using electron microscopic methods and biochemical assays that allow detection of intermediates in the process of coated vesicle formation, we have established that the elel mutant dynamin blocks coated vesicle formation at a stage after coat assembly but before the formation of sealed coated vesicles. Specifically, we conclude that dynamin is required for the constriction of coated pits and for coated vesicle budding.

While late stages in coated vesicle formation are blocked in cells overexpressing mutant dynamin, early events are unaffected. Plasma membrane specific AP2 complexes are quantitatively recruited to the cell surface and clathrin-coated lattices form properly in the mutant cell line. Receptors are concentrated into coated pits with the same sorting efficiency as in wild-type cells. The invaginated coated pits that accumulate in cells expressing mutant dynamin are indistinguishable in size and shape from those in wild-type cells. However, these invaginated coated pits fail to undergo constriction and, therefore, fail to sequester receptor-bound, biotinylated-ligands from the large exogenously added probe, avidin. The accumulation of invaginated pits at the plasma membrane is entirely consistent with the phenotype of *shibire*^{ts} flies exposed to the nonpermissive temperature, which also accumulate coated pits that remain accessible to exogenously added HRP-conjugated wheat germ agglutinin (Narita et al., 1989).

Previous evidence for a late regulated event in coated vesicle formation from the plasma membrane has been obtained in other systems. For example, endocytosis is inhibited in mitotic A431 cells by a block late in vesicle formation resulting in the accumulation of invaginated coated pits (Pypaert et al., 1987). Similarly, invaginated coated pits accumulate in ATP-depleted HeLa and K562 cells (Schmid and Carter, 1990). In perforated A431 cells, preformed flat coated pits spontaneously invaginate (Smythe et al., 1989), whereas subsequent events leading to the sequestration of ligands into constricted coated pits require cytosolic factors, ATP, and micromolar concentrations of GTP. These factors are also required for coated vesicle budding (Smythe et al., 1989; Schmid and Smythe, 1991; Carter et al., 1993). Together with the results presented here, these observations suggest that dynamin might be one cytosolic factor required for a regulated, energy-dependent step(s) late in the process of coated vesicle formation involving coated pit constriction and membrane scission.

Dynamin Specifically Blocks Coated Vesicle Formation at the Plasma Membrane

The block in coated vesicle formation was specific for vesicle budding at the plasma membrane: neither biosynthetic pathways leading to the plasma membrane or to lysosomes, nor recycling pathways from endosomes to the plasma membrane were affected. This specificity in the functional interference of mutant dynamin, even when expressed at very high levels, is comparable to that observed with small rab GTPases in vesicular transport. Each member of the rab/ypt family is exclusively involved in a specific membrane transport event in eukaryotic cells (Zerial and Stenmark, 1993; Nouffer and Balch, 1994). Strikingly, overexpression of mutant dynamin did not affect the mechanistically related event of clathrin-coated vesicle formation at the TGN. This result implies that, as for rab proteins, dynamin might have functionally related family members that function in vesicle budding at discrete intracellular locations.

Dynamin is, in fact, a member of a multigene family (Obar et al., 1990), although many family members (e.g., Mx proteins or MGMlp) have functions apparently unrelated to vesicular transport (Collins, 1991). One dynamin family member, the yeast protein VPSlp, is involved in vacuolar sorting (Vater et al., 1992), which is mediated by clathrin-coated vesicles (Wilsbach and Payne, 1993). It is, therefore, attractive to speculate that VPSlp might play an analogous role to dynamin in coated vesicle budding at the TGN.

Dynamin-1 and Dynamin-2 Are Coated Pit–associated Proteins Suggesting a Common Function

The dynamin cDNA used in these studies encodes a neuron-specific isoform of dynamin (referred to as dynamin-1) that is not expressed in HeLa cells (Warnock, D. E., J. L. Terlecky, and S. L. Schmid, manuscript submitted for publication). A second isoform, referred to as dynamin-2, which is 79% identical to dynamin-1, is ubiquitously expressed (Cook et al., 1994; Sontag et al., 1994), and probably represents the isoform detected in HtTA cells. A third isoform, referred to as dynamin-T, is exclusively expressed in the testis (Nakata et al., 1993). A subset of the monoclonal antibodies we have raised to dynamin-1 also recognize dynamin-2 (this report and Warnock et al., manuscript in preparation). Consistent with the specificity of the functional interference of elel mutant dynamin, EM immunolocalization using these antibodies has revealed that membrane-associated endogenous dynamin-2 and overexpressed dynamin-1 isoforms are both localized to the cytoplasmic surface of the plasma membrane, specifically in clathrin-coated pits. These results suggest that dynamin-1 and dynamin-2 share

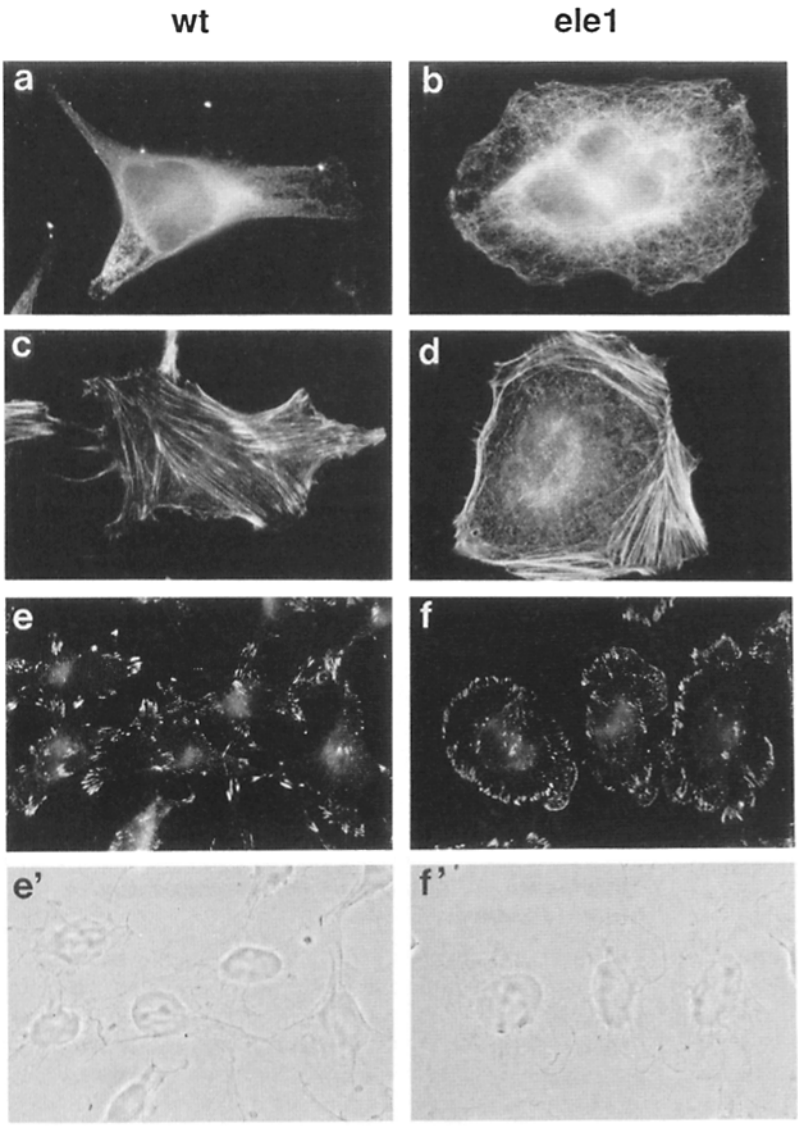

Figure 12. Alteration of cytoskeleton and cell shape in mutant dynamin cells. After induction of dynamin, wt (*a*, *c*, *e* and *e'*), and elel cells (*b*, *d*, *f*, *f'*) were fixed, permeabilized, and stained with anti-tubulin (*a* and *b*), rhodamine-phalloidin (*c* and *d*), or anti-vinculin (*e* and *f*) antibodies for indirect immunofluorescence. Phase contrast images (*e'* and *f'*) were from the same area as the anti-vinculin stain.

a saturable membrane binding site for specific targeting to plasma membrane–associated clathrin coated pits.

Targeting of Dynamin to Coated Pits

Dynamin is distinguished from other family members, including VPS1p, by a 100-aa proline-rich, highly basic COOH-terminal domain. This proline-rich "tail" is structurally related to the COOH terminus of synapsin I, which is involved in its binding both to the actin cytoskeleton and to synaptic vesicles (Benfenati et al., 1993). While a large, 188-aa deletion of the COOH terminus negates the inhibitory effects of dominant-negative mutants of dynamin, deletion of 57 aa of the 100-aa proline-rich tail of dynamin does not (Herskovits et al., 1993*a*). Proline-rich domains are common to a number of functionally diverse proteins, where they are believed to provide rigid, extended, hydrophobic surfaces that entropically and enthrapically favor rapid, high affinity binding interactions (reviewed by Williamson, 1994). These binding properties can often survive large deletions within long proline-rich sequences (Williamson, 1994). Thus these results are consistent with the hypothesis that the proline-rich tail participates in protein–protein interactions that are important for targeting dynamin to its site of action.

Both synapsin I (Benfenati et al., 1989) and dynamin (Tuma et al., 1993) bind to specific cellular membranes and interact with acidic phospholipids. For synapsin I, this interaction with acidic phospholipids occurs mainly through the NH_2-terminal domain, yet association of synapsin I to protein components on synaptic vesicles occurs via the COOH-terminal proline-rich sequences (Benfenati et al., 1989). Like the binding of synapsin I to synaptic vesicles, the saturable binding and specific targeting of dynamin to coated regions on the plasma membranes is unlikely to be mediated only by its affinity for acidic phospholipids. Dynamin-membrane association is extremely tight, requiring almost denaturing conditions for its release from crude bovine brain membrane preparations (Tuma et al., 1993; Schmid, S. L., unpublished observations). Phosphorylation of the proline-rich tail of synapsin I upon depolarization disrupts its interaction with both actin filaments and synaptic vesicles,

thereby allowing synaptic vesicle release. Interestingly, dynamin is coordinately dephosphorylated upon membrane depolarization (Robinson et al., 1993). It is tempting to speculate that phosphorylation/dephosphorylation of dynamin might similarly regulate interactions through its proline-rich domain. Identification of the membrane-binding site for dynamin and of other factors that interact with dynamin will clearly be of importance to understanding its function in coated vesicle formation.

The Dynamin GTPase Cycle and Coated Vesicle Formation

Dynamin is a cytosolic protein also associated with coated pits at the plasma membrane and with coated vesicles. Thus, it is likely that dynamin undergoes a cycle of membrane association/dissociation coupled to the cycle of nucleotide exchange and hydrolysis in carrying out its role in coated pit constriction and coated vesicle budding. How might the dynamin cycle of GTP binding and hydrolysis function in coated vesicle formation? The elel mutant has low affinity for both GTP and GDP, and it is assumed to be in the unoccupied state, yet it has similar or higher levels of membrane association than wild-type dynamin (not shown, but see van der Bliek et al., 1993). Therefore, we propose that membrane binding is independent of the GTP binding and hydrolysis activity of dynamin. Even when dramatically overexpressed, both wt and elel dynamin are selectively associated with clathrin lattices on the plasma membrane. It is interesting to compare this localization with that of AP2 "adaptor" complexes. Consistent with their role in early, "priming" events preceding clathrin assembly (Mahaffey et al., 1990; Smythe et al., 1992), APs are found on both clathrin-coated and noncoated regions of the plasma membrane (Baba, T., and S. L. Schmid, unpublished results). Together, these results are consistent with the model that coated vesicle formation begins with AP priming of membranes, followed by the assembly of clathrin into flat lattices and the recruitment of dynamin in its unoccupied or GDP-bound form to these initially planar structures.

Invaginated coated pits accumulate in cells expressing elel dynamin. Therefore, we propose that this step in coated vesicle formation is also independent of the GTP-binding and hydrolysis activity of dynamin. In contrast, the constriction of coated pits that precedes vesicle budding is blocked in elel cells. In vitro analysis of events leading to ligand sequestration demonstrated that this step required >10 μM GTP, was insensitive to GTPγS, but was inhibited by GDPβS (Carter et al., 1993). These results suggest that a GTP/GDP exchange reaction might be required to convert dynamin to its GTP-bound form for the constriction event. GTP hydrolysis is apparently not required until a later stage, either in vesicle budding or in the recycling of dynamin from coated vesicles. In this regard, Oka and Nakano (1994) have recently demonstrated that GTP hydrolysis by the Sarlp GTPase is not required for vesicle budding from the ER, but is instead required for recycling of this component from transport vesicles. We have shown that coated vesicle budding in perforated A431 cells also requires >10 μM GTP, but is sensitive to the nonhydrolyzable analogue GTPγS (Carter et al., 1993). While this might reflect the involvement of other GTPases in vesicle budding as initially proposed, it is also possible that GTP hydrolysis by dynamin is required for vesicle budding.

Fluid Phase Uptake Continues at Normal Levels after Inhibition of Receptor-Mediated Endocytosis

The conditional overexpression of mutant dynamin blocks coated vesicle formation by >80%. We assume that this pathway is of essential importance to guarantee the cells' supply of nutrients and to regulate the steady-state total surface area. The surprising observation that cells expressing mutant dynamin remained viable could be explained by the finding that fluid phase uptake continues in cells severely inhibited in clathrin-dependent endocytosis. In contrast, morphological studies in cells expressing the *shibire* mutant demonstrated that HRP uptake was potently inhibited when measured shortly after shift to the nonpermissive temperature (Koenig and Ikeda, 1983; Kessell et al., 1989). Taken together, these results suggest that a pathway for bulk-flow endocytosis was induced in compensation for the loss of clathrin-dependent endocytosis after prolonged expression of elel dynamin. Interestingly, prolonged incubation of yeast strains carrying a temperature-sensitive mutation in the clathrin heavy chain at the nonpermissive temperature also induces a compensatory pathway that relieves the vacuolar sorting defect (Seeger and Payne, 1992). It remains to be determined whether the compensatory mechanisms are similar in these cell systems. Further work involving analysis of earlier time points after the induction of expression of mutant dynamin in the stably transformed cell system will be needed to define this clathrin-independent pathway and the mechanisms by which it is induced.

Morphological Consequences of Overexpression of Mutant Dynamin

The effect of overexpression of mutant dynamin on intracellular membrane trafficking events was restricted to clathrin-coated vesicle formation at the cell surface. However, it was important to examine the ultrastructure of cells overexpressing mutant dynamin to address the issue of whether any other cellular functions were affected. Overexpression of wt dynamin did not alter cell morphology at either the light or electron microscopic levels. Membranous structures that accumulated in elel cells were apparently derived from the plasma membrane and other endocytic organelles. We have observed HtTA cells 24–48 h after induction of elel dynamin, compared to the rapid and synchronous temperature-sensitive effect of the *shibire* mutation. Therefore, in our system, direct and indirect consequences of mutant dynamin expression can not be distinguished. However, since our results were generally consistent with morphological studies on *shibire*^{ts} flies (Kosaka and Ikeda, 1983*a*, 1983*b*; Narita et al., 1989), we conclude that perturbations caused by overexpression of elel dynamin were restricted to the endocytic pathway in mammalian cells.

The most readily detectable phenotype resulting from induction of elel dynamin was that the cells became flattened, extended their cytoplasm, and the normally longitudinal stress fibers were reorganized to form circumferentially distributed actin filaments. These phenotypic changes might reflect an additional function for dynamin. For example, like synapsin-I, dynamin may interact directly with actin filaments through its proline-rich tail (Benfenati et al., 1993). However, we believe these effects are more likely an indirect consequence of the inhibition of receptor-mediated endocytosis for two reasons. First, dynamin was uniformly dis-

tributed in punctate structures on the basement membranes of elel HtTA cells showing no relationship to the peripheral distribution of actin filaments or vinculin-positive adhesion plaques. Second, identical morphological changes have been reported in human fibroblasts after inhibition of receptor-mediated endocytosis by completely different mechanisms, namely K^+ depletion and cytosolic acidification (Altankov and Grinnell, 1993). These authors concluded that receptor-mediated endocytosis (perhaps of integrin family members) might be important for the regulation of cell adhesion and the establishment of cell polarity.

Several developmental phenotypes are associated with the *shibire* mutation in *Drosophila*, including growth cone formation, neurite development, cell adhesion, and differentiation (Buzin et al., 1978; Poodry and Edgar, 1979; Kim and Wu, 1987). It is, therefore, attractive to speculate that dynamin plays a key role in linking endocytosis and signal transduction, not only through known pathways involving tyrosine kinase growth factor receptors, but also through novel interactions with components of the extracellular matrix. While a requirement for dynamin function in the endocytic machinery may be sufficient to explain these other phenotypes, it is too early to dismiss the possibility of alternate or additional functions for dynamin.

In summary, these studies have provided strong evidence for the specificity of dynamin's function in coated vesicle formation, and they have provided the first working model for the role of the dynamin GTPase cycle in this process. Much remains to be understood. Studies are now in progress to generate other mutations that arrest dynamin in its GTP-bound and GDP-bound conformations so that the biochemical and morphological approaches described here can be used to identify the intermediates that accumulate in cells expressing these mutants. Characterization of these intermediates will help refine our model for dynamin's function in vesicle formation and should more precisely define dynamin's role as regulator or effector in the process of vesicle constriction and budding.

We would like to thank Drs. M. Gossen and H. Bujard for kindly providing the HtTA cells and the plasmid pUHD10-3, Drs. Alexander van der Bliek and Dalia Resnitzky for helpful discussions, Jeanne Matteson for technical assistance, Dr. Jenny Hinshaw for providing bovine brain coated vesicles, Dr. Cheng-Ming Chang for thin-section EM preparations, George Klier for confocal microscopy, and Michael McCaffery for cryo-ultrathin section and immunogold staining, which was performed in the EM Core Facility, run by Dr. M. G. Farquhar and supported by National Cancer Institute grant CA58689.

This work was supported by National Institutes of Health grant GM42445 and a grant from the Lucille P. Markey Charitable Trust to S. L. Schmid. S. L. Schmid is a Lucille P. Markey Scholar. H. Damke was supported by a fellowship from the Deutsche Forschungsgemeinschaft. This is manuscript number 8777-CB from The Scripps Research Institute.

Received for publication 14 June 1994 and in revised form 22 July 1994.

References

Ahle, S., A. Mann, U. Eichelsbacher, and E. Ungewickell. 1988. Structural relationships between clathrin assembly proteins from the Golgi and the plasma membrane. *EMBO (Eur. Mol. Biol. Organ.) J.* 7:919–929.

Altankov, G., and F. Grinnell. 1993. Depletion of intracellular potassium disrupts coated pits and reversibly inhibits cell polarization during fibroblast spreading. *J. Cell Biol.* 120:1449–1459.

Balch, W. E., J. M. McCaffery, H. Plutner, and M. G. Farquhar. 1994. Vesicular stomatitis virus glycoprotein is sorted and concentrated during export from the endoplasmic reticulum. *Cell.* 76:841–852.

Benfenati, F., P. Greengard, J. Brunner, and M. Bähler. 1989. Interactions of synapsin I with small synaptic vesicles: distinct sites in synapsin I bind to vesicle phospholipids and vesicle proteins. *J. Cell Biol.* 108:1863–1872.

Benfenati, F., F. Valtorta, M. C. Rossi, F. Onofri, T. Sihra, and P. Greengard. 1993. Interactions of Synapsin I with phospholipids: possible role in synaptic vesicle clustering and in the maintenance of bilayer structures. *J. Cell Biol.* 123:1845–1855.

Besterman, J. M., J. A. Airhart, R. C. Woodworth, and R. B. Low. 1981. Exocytosis of pinocytosed fluid in cultured cells: kinetic evidence for rapid turnover and compartmentation. *J. Cell Biol.* 91:716–727.

Burnette, W. N. 1981. "Western blotting": electrophoretic transfer of proteins from sodium dodecyl sulfate-polyacrylamide gels to unmodified nitrocellulose and radiographic detection with antibody and radioiodinated protein A. *Anal. Biochem.* 112:195–203.

Buzin, C. H., S. A. Dewhurst, and R. L. Seecof. 1978. Temperature sensitivity of muscle and neuron differentiation in embryonic cultures from the *Drosophila* mutant *shibire*^{ts1}. *Dev. Biol.* 66:442–456.

Carter, L. L., T. E. Redelmeier, L. A. Woollenweber, and S. L. Schmid. 1993. Multiple GTP-binding proteins participate in clathrin-coated vesicle-mediated endocytosis. *J. Cell Biol.* 120:37–45.

Chen, M. S., R. A. Obar, C. C. Schroeder, T. W. Austin, C. A. Poodry, S. C. Wadsworth, and R. B. Vallee. 1991. Multiple forms of dynamin are encoded by *shibire*, a *Drosophila* gene involved in endocytosis. *Nature (Lond.).* 351: 583–586.

Ciechanover, A., A. L. Schwartz, A. Dautry-Varsat, and H. F. Lodish. 1983. Kinetics of internalization and recycling of transferrin and the transferrin receptor in a human hepatoma cell line. *J. Biol. Chem.* 258:9681–9689.

Collins, C. A. 1991. Dynamin: a novel microtubule-associated GTPase. *Trends Cell Biol.* 1:57–60.

Cook, T. A., R. Urrutia, and M. A. McNiven. 1994. Identification of dynamin 2, an isoform ubiquitously expressed in rat tissues. *Proc. Natl. Acad. Sci. USA.* 91:644–648.

Damke, H., M. Gossen, S. Freundlieb, H. Bujard, and S. L. Schmid. 1995. Tightly regulated and inducible expression of a dominant interfering dynamin mutant in stably transformed HeLa cells. *Methods Enzymol.* In press.

de la Luna, S., I. Soria, D. Pulido, J. Ortin, and A. Jimenez. 1988. Efficient transformation of mammalian cells with constructs containing a puromycin-resistance marker. *Gene (Amst.).* 62:121–126.

Gieselmann, V., R. Pohlmann, A. Hasilik, and K. von Figura. 1983. Biosynthesis and transport of cathepsin D in cultured human fibroblasts. *J. Cell Biol.* 97:1–5.

Gilmore, R. 1991. The protein translocation apparatus of the rough endoplasmic reticulum, its associated proteins, and the mechanism of translocation. *Curr. Opin. Cell Biol.* 3:580–584.

Gossen, M., and H. Bujard. 1992. Tight control of gene expression in mammalian cells by tetracycline-responsive promoters. *Proc. Natl. Acad. Sci. USA.* 89:5547–5551.

Gout, I., R. Dhand, I. D. Hiles, M. J. Fry, G. Panayotou, P. Das, O. Truong, N. F. Totty, J. Hsuan, G. W. Booker, I. D. Campbell, and M. D. Waterfield. 1993. The GTPase dynamin binds to and is activated by a subset of SH3 domains. *Cell.* 75:25–36.

Griffiths, G., R. Black, and M. Marsh. 1989. A quantitative analysis of the endocytic pathway in baby hamster kidney cells. *J. Cell Biol.* 109:2703–2720.

Grigliatti, T. A., L. Hall, R. Rosenbluth, and D. T. Suzuki. 1973. Temperature-sensitive mutations in *Drosophila melanogaster.* XV. Selection of immobile adults. *Mol. Gen. Genet.* 120:107–114.

Herskovits, J. S., C. C. Burgess, R. A. Obar, and R. B. Vallee. 1993*a*. Effects of mutant rat dynamin on endocytosis. *J. Cell Biol.* 122:565–578.

Herskovits, J. S. C., H. S. Shpetner, C. C. Burgess, and R. B. Vallee. 1993*b*. Microtubules and Src homology 3 domains stimulate the dynamin GTPase via its C-terminal domain. *Proc. Natl. Acad. Sci. USA.* 90:11468–11472.

Heuser, J., and L. Evans. 1980. Three-dimensional visualization of coated vesicle formation in fibroblasts. *J. Cell Biol.* 84:560–583.

Kessell, I., B. D. Holst, and T. F. Roth. 1989. Membrane intermediates in endocytosis are labile, as shown in a temperature-sensitive mutant. *Proc. Natl. Acad. Sci. USA.* 86:4968–4972.

Kim, Y.-T., and C.-F. Wu. 1987. Reversible blockage of neurite development and growth cone formation in neuronal cultures of a temperature sensitive mutant of *Drosophila. J. Neurosci.* 7:3245–3255.

Koenig, J. H., and K. Ikeda. 1989. Disappearance and reformation of synaptic vesicle membrane upon transmitter release observed under reversible blockage of membrane retrieval. *J. Neurosci.* 11:3844–3860.

Koenig, J. H., and K. Ikeda. 1990. Transformational process of the endosomal compartment in nephrocytes of *Drosophila melanogaster. Cell Tissue Res.* 262:233–244.

Kornfeld, S., and I. Mellman. 1989. The biogenesis of lysosomes. *Annu. Rev. Cell Biol.* 5:483–525.

Kosaka, T., and K. Ikeda. 1983*a*. Possible temperature-dependent blockage of synaptic vesicle recycling induced by a single gene mutation in *Drosophila. J. Neurobiol.* 14:207–225.

Kosaka, T., and K. Ikeda. 1983*b*. Reversible blockage of membrane retrieval and endocytosis in the garland cell of the temperature-sensitive mutant of *Drosophila melanogaster, shibire*^{ts1}. *J. Cell Biol.* 97:499–507.

Lamaze, C., T. Baba, T. E. Redelmeier, and S. L. Schmid. 1993. Recruitment

of epidermal growth factor receptor and transferrin receptors into coated pits in vitro: differing biochemical requirements. *Mol. Biol. Cell.* 4:715–727.

Maeda, K., T. Nakata, Y. Noda, R. Sato-Yoshitake, and N. Hirokawa. 1992. Interaction of dynamin with microtubules: its structure and GTPase activity investigated by using highly purified dynamin. *Mol. Biol. Cell.* 3:1181–1194.

Mahaffey, D. T., J. S. Peeler, F. M. Brodsky, and R. G. W. Anderson. 1990. Clathrin-coated pits contain an integral membrane protein that binds the AP-2 subunit with high affinity. *J. Biol. Chem.* 265:16514–16520.

Marsh, M., S. L. Schmid, H. Kern, E. Harms, P. Male, I. Mellman, and A. Helenius. 1987. Rapid analytical and preparative isolation of functional endosomes by free flow electrophoresis. *J. Cell Biol.* 104:875–886.

Moore, M. S., D. T. Mahaffey, F. M. Brodsky, and R. G. W. Anderson. 1987. Assembly of clathrin-coated pits onto purified plasma membranes. *Science (Wash. DC).* 236:558–563.

Nakata, T., A. Iwamoto, Y. Noda, R. Takemura, H. Yoshikura, and N. Hirokawa. 1991. Predominant and developmentally regulated expression of dynamin in neurons. *Neurons.* 7:461–469.

Nakata, T., R. Takemura, and N. Hirokawa. 1993. A novel member of the dynamin family of GTP-binding proteins is expressed specifically in the testis. *J. Cell Sci.* 105:1–5.

Narita, K., T. Tsuruhara, J. H. Koenig, and K. Ikeda. 1989. Membrane pinch-off and reinsertion observed in living cells of *Drosophila*. *J. Cell Physiol.* 141:383–391.

Nuoffer, C., and W. E. Balch. 1994. GTPases: multifunctional molecular switches regulating vesicular traffic. *Annu. Rev. Biochem.* 63:949–990.

Obar, R. A., C. A. Collins, J. A. Hammarback, H. S. Shpetner, and R. B. Vallee. 1990. Molecular cloning of the microtubule-associated mechanochemical enzyme dynamin reveals homology with a new family of GTP-binding proteins. *Nature (Lond.).* 347:256–261.

Oka, T., and A. Nakano. 1994. Inhibition of GTP hydrolysis by Sar1p causes accumulation of vesicles that are a functional intermediate of the ER-to Golgi transport in yeast. *J. Cell Biol.* 124:425–434.

Omary, M. B., and I. S. Trowbridge. 1981. Biosynthesis of the human transferrin receptor in cultured cells. *J. Biol. Chem.* 256:12888–12892.

Pai, E. F., U. Krengel, G. A. Petsko, R. S. Goody, W. Kabsch, and A. Wittinghofer. 1990. Refined crystal structure of the triphosphate conformation of H-ras p21 at 1.35 A resolution: implication for the mechanism of GTP hydrolysis. *EMBO (Eur. Mol. Biol. Organ.) J.* 9:2351–2359.

Pearse, B. M. F. 1975. Coated vesicles from pig brain: purification and biochemical characterization. *J. Mol. Biol.* 97:93–98.

Poodry, C. A., and L. Edgar. 1979. Reversible alterations in the neuromuscular junctions of *Drosophila melanogaster* bearing a temperature-sensitive mutation, *shibire*. *J. Cell Biol.* 81:520–527.

Pypaert, M., J. M. Lucocq, and G. Warren. 1987. Coated pits in interphase and mitotic A431 cells. *Eur. J. Cell Biol.* 45:23–29.

Resnitzky, D., M. Gossen, H. Bujard, and S. I. Reed. 1994. Acceleration of the G_1/S phase transition by expression of cyclins D1 and E with an inducible system. *Mol. Cell Biol.* 14:1669–1679.

Robinson, M. S. 1992. Adaptins. *Trends Cell Biol.* 2:293–297.

Robinson, P. J., J.-M. Sontag, J.-P. Liu, E. M. Fykse, C. Slaughter, H. McMahon, and T. C. Südhof. 1993. Dynamin GTPase regulated by protein kinase C phosphorylation in nerve terminals. *Nature (Lond.).* 365:163–166.

Sambrook, J., E. F. Fritsch, and T. Maniatis. 1989. Molecular Cloning. A Laboratory Manual. Cold Spring Harbor Laboratory Press, Cold Spring Harbor, NY. 545 pp.

Sanan, D. A., and R. G. W. Anderson. 1991. Simultaneous visualization of LDL receptor distribution and clathrin lattices on membranes torn from the upper surface of cultured cells. *J. Histochem. Cytochem.* 39:1017–1024.

Scaife, R., and R. L. Margolis. 1990. Biochemical and immunochemical analysis of rat brain dynamin interaction with microtubules and organelles in vivo and vitro. *J. Cell Biol.* 111:3023–3033.

Schmid, S. L., and L. L. Carter. 1990. ATP is required for receptor-mediated endocytosis in intact cells. *J. Cell Biol.* 111:2307–2318.

Schmid, S. L., and E. Smythe. 1991. Stage-specific assays for coated pit formation and coated vesicle budding in vitro. *J. Cell Biol.* 114:869–880.

Schmid, S. L. 1993. Coated-vesicle formation in vitro: conflicting results using different assays. *Trends Cell Biol.* 3:145–148.

Seeger, M., and G. S. Payne. 1992. A role for clathrin in the sorting of vacuolar proteins in the Golgi complex of yeast. *EMBO (Eur. Mol. Biol. Organ.) J.* 11:2811–2818.

Shpetner, H. S., and R. B. Vallee. 1989. Identification of dynamin, a novel mechanochemical enzyme that mediates interactions between microtubules. *Cell.* 59:421–432.

Shpetner, H. S., and R. B. Vallee. 1992. Dynamin is a GTPase stimulated to high levels of activity by microtubules. *Nature (Lond.).* 355:733–735.

Smythe, E., M. Pypaert, J. Lucocq, and G. Warren. 1989. Formation of coated vesicles from coated pits in broken A431 cells. *J. Cell Biol.* 108:843–853.

Smythe, E., L. L. Carter, and S. L. Schmid. 1992*a*. Cytosol- and clathrin-dependent stimulation of endocytosis in vitro by purfiied adaptors. *J. Cell Biol.* 119:1163–1171.

Smythe, E., T. E. Redelmeier, and S. L. Schmid. 1992*b*. Receptor-mediated endocytosis in semiintact cells. *Methods Enzymol.* 219:223–234.

Sontag, J.-M., E. M. Fykse, Y. Ushkaryov, J.-P. Liu, P. J. Robinson, and T. C. Südhof. 1994. Differential expression and regulation of multiple dynamins. *J. Biol. Chem.* 269:4547–4554.

Trowbridge, I. S., J. F. Collawn, and C. R. Hopkins. 1993. Signal-dependent membrane protein trafficking in the endocytic pathway. *Annu. Rev. Cell Biol.* 9:129–161.

Tsuruhara, T., J. H. Koenig, and K. Ikeda. 1990. Synchronized endocytosis studied in the oocyte of a temperature-sensitive mutant of *Drosophila melanogaster*. *Cell Tissue Res.* 259:199–207.

Tuma, P. L., M. C. Stachniak, and C. A. Collins. 1993. Activation of dynamin GTPase by acidic phospholipids and endogenous rat brain vesicles. *J. Biol. Chem.* 268:17240–17246.

Vallee, R. B. 1992. Dynamin: motor protein or regulatory GTPase. *J. Muscle Res. Cell Motil.* 13:493–496.

van der Bliek, A. M., and E. M. Meyerowitz. 1991. Dynamin-like protein encoded by the *Drosophila shibire* gene associated with vesicular traffic. *Nature (Lond.).* 351:411–414.

van der Bliek, A. M., T. E. Redelmeier, H. Damke, E. J. Tisdale, E. M. Meyerowitz, and S. L. Schmid. 1993. Mutations in human dynamin block an intermediate stage in coated vesicle formation. *J. Cell Biol.* 122:553–563.

van Deurs, B., W. O. Petersen, S. Olsnes, and K. Sandvig. 1989. The ways of endocytosis. *Int. Rev. Cytol.* 117:131–177.

Vater, C. A., C. K. Raymond, K. Ekena, I. Howald-Stevenson, and T. H. Stevens. 1992. The VPS1 protein, a homologue of dynamin required for vacuolar protein sorting in *Saccharomyces cerevisiae*, is a GTPase with two functionally separable domains. *J. Cell Biol.* 119:773–786.

Williamson, M. P. 1994. The structure and functions of proline-rich regions in proteins. *Biochem. J.* 297:249–260.

Wilsbach, K., and G. S. Payne. 1993. Vps1p, a member of the dynamin GTPase family, is necessary for Golgi membrane protein retention in *Saccharomyces cerevisiae*. *EMBO (Eur. Mol. Biol. Organ.) J.* 12:3049–3059.

Wilson, I. A., H. L. Niman, R. A. Houghten, A. R. Cherenson, M. L. Connolly, and R. A. Lerner. 1984. The structure of an antigenic determinant in a protein. *Cell.* 37:767–778.

Zerial, M., and H. Stenmark. 1993. Rab GTPases in vesicular transport. *Curr. Opin. Cell Biol.* 5:613–620.